# COMMUNICATION LINK PERFORMANCE EVALUATION FOR GEOSTATIONARY SATELLITE VERSUS LOW EARTH ORBIT SATELLITE NETWORK IN TROPICAL REGION

BY

HAZRUL HAFIZ B. ABDUL SHUKUR

INTERNATIONAL ISLAMIC UNIVERSITY MALAYSIA

2026

# COMMUNICATION LINK PERFORMANCE EVALUATION FOR GEOSTATIONARY SATELLITE VERSUS LOW EARTH ORBIT SATELLITE NETWORK IN TROPICAL REGION

BY

HAZRUL HAFIZ B. ABDUL SHUKUR

A dissertation submitted in fulfillment of the requirement for the Master of Science in Engineering

Kulliyyah of Engineering
International Islamic University Malaysia

JUNE 2026

# ABSTRACT

Latency is a key performance factor for satellite internet, especially for real-time applications like web browsing, video calls, Virtual Private Network (VPN), and remote access used in rural, maritime, emergency, and military environments. While Geostationary (GEO) High Throughput System (HTS) systems still experience high latency due to their orbital altitude, Starlink's Low Earth Orbit (LEO) constellation now offers globally available low-latency, high-bandwidth satellite internet. Despite their high-speed benefits, both HTS systems in GEO and LEO are using Ku-band which is highly susceptible to rain-induced signal attenuation, particularly in regions with heavy rainfall such as the tropics and equatorial countries. The rain attenuation at Ku-band not only weakens the radio frequency signals but also increases real time latency in the satellite communication link. This research aims to determine the latency of HTS satellites in LEO and GEO induced by rain and evaluate its performance under heavy rainfall conditions. This study uses real satellite link paid services from Société Européenne des Satellites (SES) operator from Luxembourg, SES-12 a geostationary HTS located at 95° east and Starlink LEO constellation operated by Starlink Services a subsidiary of American space company, SpaceX for rain-induced latency performance assessment. A 1.2m VSAT terminal for SES-12 and a Starlink terminal were installed to measure and record latency continuously for six months at the same location with a collocated rain gauge to measure rainfall rate. Site-specific latency datasets were collected to evaluate the Round Trip Time (RTT) using Ku-band link under various rainfall intensities for both satellite services. The empirical measurements were further developed into rain-induced latency correlations, using power law and logarithmic based equations that directly relate to rainfall rate for both satellite systems. These new relationships capture the nominal and tail latency behaviors, representing the normal operating conditions and the degraded latency performance during severe rain-fade conditions, respectively. The results show that the SES-12 GEO terminal latency ranges from 600 ms to 3,000 ms, while the LEO Starlink terminal maintains a much lower latency between 20 ms and 100 ms. Starlink achieved higher link availability (99.6 %) compared to 94 % for SES-12 in the same tropical environment. The findings indicate that extreme rainfall significantly impacts the GEO link, causing prolonged signal degradation and delay expansion, whereas the LEO link remains less affected due to its low-orbit architecture and dynamic satellite switching capability.

**Keywords:** Low Earth Orbit (LEO), Geostationary Earth Orbit (GEO), Rain-Induced Latency, Ku-Band Satellite Communications, Tropical Regions, Empirical Measurements, Link Availability.

# ملخص البحث


تُعدّ فترة التأخير (Latency) أحد أهم مؤشرات الأداء في خدمات الإنترنت عبر الأقمار الصناعية، ولا سيما للتطبيقات الآنية مثل تصفح الويب، ومؤتمرات الفيديو، والشبكات الافتراضية الخاصة(VPN) ، والوصول عن بُعد في البيئات الريفية والبحرية وحالات الطوارئ والعمليات العسكرية. وعلى الرغم من أن الأقمار الصناعية عالية السعة (HTS) في المدار الثابت بالنسبة للأرض (GEO) توفر تغطية واسعة، فإن ارتفاعها المداري الكبير يؤدي بطبيعته إلى زمن تأخير مرتفع.في المقابل، توفر منظومات الأقمار الصناعية في المدار الأرضي المنخفض(LEO) ، مثل شبكة ستارلينك، اتصالاً عالمياً يتميز بانخفاض زمن التأخير وارتفاع سعة نقل البيانات. ومع ذلك، فإن كلا النظامين العاملين ضمن نطاق التردد Ku-band يتأثران بشكل ملحوظ بالتوهين الناتج عن الأمطار، خاصةً في المناطق الاستوائية ذات معدلات الهطول المرتفعة.تهدف هذه الدراسة إلى تقييم تأثير الأمطار على أداء زمن التأخير في شبكات الأقمار الصناعية من نوعي GEO و LEOباستخدام خدمتي SES-12 وستارلينك. وقد تم تركيب محطة طرفية ذات فتحة صغيرة جداً (VSAT) بقطر 1.2 متر لخدمةSES-12 ، بالإضافة إلى محطة ستارلينك، في موقع واحد مزود بمقياس للأمطار، حيث جُمعت البيانات بشكل مستمر لمدة ستة أشهر . وتم تحليل قياسات زمن الرحلة ذهاباً وإياباً (RTT) تحت مستويات مختلفة من شدة هطول الأمطار، كما تم تطوير نماذج تجريبية تعتمد على علاقات أسية ولوغاريتمية لوصف سلوك زمن التأخير في الظروف التشغيلية الاعتيادية وحالات التوهين الشديد الناتج عن الأمطار.

أظهرت النتائج أن زمن التأخير في نظام SES-12 تراوح بين 600 و3000 مللي ثانية، في حين حافظ نظام ستارلينك على زمن تأخير منخفض تراوح بين 20 و100 مللي ثانية. كما حقق ستارلينك نسبة إتاحة للوصلة بلغت 99.6% مقارنةً بـ 94% لنظام.SES-12 وتؤكد النتائج أن الأمطار الغزيرة تؤثر بشكل كبير على أداء الأقمار الصناعية في المدار الثابت بالنسبة للأرض، بينما تتمتع أنظمة المدار الأرضي المنخفض بقدرة أعلى على مقاومة تأثيرات الأمطار بفضل بنيتها المدارية المنخفضة وآلية التبديل الديناميكي بين الأقمار الصناعية، مما يجعلها أكثر ملاءمةً للتطبيقات الحساسة لزمن التأخير في البيئات الاستوائية.

# APPROVAL PAGE

I certify that I have supervised and read this study and that in my opinion, it conforms to acceptable standards of scholarly presentation and is fully adequate, in scope and quality, as a dissertation for the degree of Master of Science in Engineering.

…….
Yasser Asrul bin Ahmad
Supervisor

…….
Khairayu Badron
Co-Supervisor

I certify that I have read this study and that in my opinion it conforms to acceptable standards of scholarly presentation and is fully adequate, in scope and quality, as a dissertation for the degree of Master of Science in Engineering.

…….
Ahmad Fadzil Ismail
Internal Examiner

…….
Mardeni Roslee
External Examiner

This dissertation was submitted to the Department of Electrical and Computer Engineering and is accepted as a fulfilment of the requirement for the Master of Science in Engineering.

…….
Othman Omran Khalifa
Head, Department of Electrical and Computer Engineering

This dissertation was submitted to the Kulliyyah of Engineering and is accepted as a fulfillment of the requirement for the Master of Science in Engineering.

…….
Khairul Azami Bin Sidek
Dean, Kulliyyah of Engineering

# DECLARATION

I hereby declare that this dissertation is the result of my own investigations, except where otherwise stated. I also declare that it has not been previously or concurrently submitted as a whole for any other degrees at IIUM or other institutions.

Hazrul hafiz Abdul Shukur

Signature…… Date……01.06.2026……

**INTERNATIONAL ISLAMIC UNIVERSITY MALAYSIA**

**DECLARATION OF COPYRIGHT AND AFFIRMATION OF FAIR USE OF UNPUBLISHED RESEARCH**

**COMMUNICATION LINK PERFORMANCE EVALUATION FOR GEOSTATIONARY SATELLITE VERSUS LOW EARTH ORBIT SATELLITE NETWORK IN TROPICAL REGION**

I declare that the copyright holder of this thesis/dissertation is Hazrul Hafiz bin Abdul Shukur.

Copyright © 2026 Hazrul Hafiz bin Abdul Shukur. All rights reserved.

No part of this unpublished research may be reproduced, stored in a retrieval system, or transmitted, in any form or by any means, electronic, mechanical, photocopying, recording or otherwise without prior written permission of the copyright holder except as provided below

1. Any material contained in or derived from this unpublished research may only be used by others in their writing with due acknowledgement.

2. IIUM or its library will have the right to make and transmit copies (print or electronic) for institutional and academic purpose.

3. The IIUM library will have the right to make, store in a retrieval system and supply copies of this unpublished research if requested by other universities and research libraries.

By signing this form, I acknowledged that I have read and understand the IIUM Intellectual Property Right and Commercialization policy.

Affirmed by Hazrul Hafiz Abdul Shukur

…… …… 01.06.2026

Signature Date

# ACKNOWLEDGEMENTS

All praises be to **Allah SWT, the Most Gracious and Most Merciful**, for granting me the strength, guidance, and countless opportunities to complete this dissertation. His grace, mercy, and blessings have been my constant source of support throughout this MSc journey, making this achievement possible.

I would like to express my deepest gratitude to my supervisor, **Ir. Dr. Yasser Ahmad**, for his unwavering support, encouragement, and invaluable guidance throughout my research. His vast knowledge, patience, and wisdom have been instrumental in shaping my understanding and driving me toward the successful completion of this study. My sincere appreciation also extends to my co-supervisors, **Ir. Dr. Khairayu bt Badron**, whose insightful guidance, assistance, and constructive discussions have played a crucial role in this journey. Their unwavering encouragement has motivated me to persevere and complete this research.

This achievement is dedicated to my beloved family, whose unwavering faith in my capabilities and relentless support have been my greatest motivation. Their encouragement and sacrifices have been the foundation of my perseverance, and for that, I am forever grateful.

Lastly, I extend my heartfelt appreciation to my friends and extended family, who have provided their support in countless ways be it financial assistance, time, or moral encouragement. Their unwavering belief in me has been a pillar of strength throughout this journey, and I truly cherish their presence in my life.

With deep gratitude, I thank each one who has contributed to this journey, directly or indirectly. This achievement would not have been possible without your support. Once again, we glorify Allah for His endless mercy on us, one of which is enabling us to successfully round off the efforts of writing this thesis. Alhamdulillah

# TABLE OF CONTENTS


Abstract ..... ii
Abstract in Arabic ..... iii
Approval Page ..... iv
Declaration ..... vi
Copyright ..... vii
Acknowledgements ..... viii
Table of Contents ..... iix
List of Tables ..... xi
List of Figures ..... xii
List of Abbreviation ..... xiv
List of Symbols ..... xv

**CHAPTER ONE: INTRODUCTION ..... 1**
1.1 Background of the Study ..... 1
1.2 Problem Statement ..... 4
1.3 Purpose of the Study ..... 5
1.3.1 Focus on Two Satellite Systems ..... 6
1.3.2 Challenges in Tropical Regions ..... 6
1.4 Research Objectives ..... 7
1.5 Research Scope ..... 8

**CHAPTER TWO: LITERATURE REVIEW ..... 9**
2.1 Overview ..... 9
2.2 HTS Satellite System Overview ..... 9
2.2.1 HTS in Geostationary Orbit ..... 10
2.2.2 HTS in Low Earth Orbit(LEO) ..... 11
2.3 Rainfall Effect in Satellite Communication Link ..... 13
2.3.1 Rain Type and its Effect in Tropical Regions ..... 13
2.3.2 Rain Attenuation for Satellite Communication Link ..... 14
2.3.3 ACM Introduce to Reduce Attenuation but not Latency Impact ..... 16
2.4 Latency in Satellite Services ..... 17
2.4.1 Latency Known as Round-Trip Time (RTT) ..... 18
2.4.1.1 Data Transmission and Processing Delay ..... 18
2.4.1.2 Experimentally Measured Latency ..... 18
2.4.2 Latency Impacting on Satellite Link Performance ..... 19
2.4.2.1 Latency Tail in Satellite Services ..... 19
2.5 Summary ..... 23

**CHAPTER THREE: METHODOLOGY ..... 24**
3.1 Overview ..... 24
3.2 Satellite Technology in Tropics Climate ..... 24
3.3 Onsite Measurement and Data Collection ..... 25

3.4 Latency Tail Analysis ....28
3.4.1 Latency Tail Interpretation ....28
3.4.2 Latency Tail Visualization ....29
3.4.3 Latency Tail Interpretation and Implications ....30
3.5 Curve Fitting Scenario and Correlation ....30
3.6 Summary ....31

**CHAPTER FOUR: RESULT AND DISCUSSION ....32**
4.1 Overview ....32
4.2 Effects of Rain on Latency ....33
4.2.1 Rain Conditions ....33
4.2.2 Clear sky ....35
4.3 CDF Analysis of Rain Rate ....36
4.4 CDF Analysis of Latency ....38
4.5 Performance Comparison ....42
4.6 Latency Tail Analysis ....43
4.6.1 LEO Starlink Terminal (Low-Earth Orbit) ....46
4.6.2 SES-12 GEO HTS VSAT Terminal (Geostationary Orbit) ....46
4.7 Equation and Correlation ....47
4.7.1 Rainfall Rate Logarithmic Curve Fit ....47
4.7.2 Rainfall Rate correlation with SES-12 GEO HTS Nominal ....49
4.7.3 Rainfall Rate correlation with SES-12 GEO HTS Tail ....51
4.7.4 Rainfall Rate correlation with Starlink LEO Latency Nominal ....53
4.7.5 Rainfall Rate correlation with Starlink LEO Latency Tail ....55
4.8 Summary of Major Finding ....57
4.8.1 GEO Latency Characteristics (SES-12) ....57
4.8.2 LEO Starlink Latency Characteristics ....58
4.8.3 Rain Induced Latency Correlation ....58

**CHAPTER FIVE: CONCLUSION ....60**
5.1 Conclusion ....60
5.2 Practical Implication ....62

**REFERENCES ....64**

# LIST OF TABLES


| | | |
|---|---|---|
| Table 1.1 | LEO Satellite specifications | 6 |
| Table 1.2 | GEO HTS Satellite specifications | 6 |
| Table 1.3 | Challenges for Rain induce Latency impacting Satellite link | 7 |
| Table 2.1 | Comparison between SES12 and Starlink specifications | 12 |
| Table 2.2 | Satellite Latency and Distance Comparison GEO, MEO and LEO | 21 |
| Table 2.3 | Summary of literature review | 22 |
| Table 4.1 | Summary of site availability performance evaluation | 43 |
| Table 4.2 | Latency measurement categories from measured data | 45 |
| Table 4.3 | Rain induces latency correlation | 58 |

# LIST OF FIGURES


| | | |
|---|---|---|
| Figure 1.1 | East and South Asia Precipitation MAP | 3 |
| Figure 1.2 | Box plot of rainfall distribution of each country | 4 |
| Figure 2.1 | SES-12 satellite with malaysia footprints | 11 |
| Figure 2.2 | Starlink satellites and footprints | 12 |
| Figure 2.3 | Satellite communication link propagation loss | 15 |
| Figure 2.4 | Modulation technique flow versus SNR | 17 |
| Figure 2.5 | CDF of GEO Satellite with latency tail | 21 |
| Figure 3.1 | Onsite experimental arrangement for Starlink | 26 |
| Figure 3.2 | Onsite experimental arrangement for SES-12 GEO HTS | 27 |
| Figure 3.3 | Customized command for automated latency capturing | 28 |
| Figure 3.4 | Flow Chart for Automated Latency Script | 29 |
| Figure 4.1 | A Rain Event occurred on 22 August 2024 for the SES-12 GEO HTS | 33 |
| Figure 4.2 | A Rain Event occurred on 22 August 2024 for the Starlink LEO | 34 |
| Figure 4.3 | A Rain Event occurred on 23 August 2024 for the SES-12 GEO HTS | 34 |
| Figure 4.4 | A Rain Event occurred on 23 August 2024 for the Starlink LEO | 35 |
| Figure 4.5 | A clear sky event occurred on 5 December 2024 for the SES-12 GEO | 36 |
| Figure 4.6 | A clear sky event occurred on 5 December 2024 for the Starlink LEO | 36 |
| Figure 4.7 | CDF Analysis of Rainfall Rate (monthly) | 37 |
| Figure 4.8 | CDF Analysis of Rainfall Rate (aggregated) | 37 |
| Figure 4.9 | CDF Analysis of latency for Starlink LEO (monthly) | 39 |
| Figure 4.10 | CDF Analysis of latency for Starlink LEO (aggregated) | 40 |
| Figure 4.11 | CDF Analysis of latency for SES-12 GEO HTS (monthly) | 41 |
| Figure 4.12 | CDF Analysis of latency for SES-12 GEO HTS (aggregated) | 41 |
| Figure 4.13 | Monthly timeout and site availability | 42 |
| Figure 4.14 | Latency tail SES-12 GEO HTS | 44 |
| Figure 4.15 | Latency tail Starlink LEO | 45 |
| Figure 4.16 | Rainfall Rate Logarithmic Curve Fit | 48 |
| Figure 4.17 | SES-12 GEO HTS Tail Power Curve Nominal | 50 |

Figure 4.18 SES-12 GEO HTS Tail Power Curve Fit 52
Figure 4.19 Starlink LEO Nominal Power Curve Fit 54
Figure 4.20 Starlink LEO Tail Power Curve Fit 56

# LIST OF ABBREVIATION

| | |
|---|---|
| HTS | High Throughput Satellite |
| IoT | Internet of Things |
| M2M | Machine to Machine |
| GEO | Geostationary Earth Orbit |
| LEO | Low Earth Orbit |
| MEO | Medium Earth Orbit |
| ITU | International Telecommunication Union |
| SNR | Signal-to-Noise Ratio |
| BER | Bit Error Rate |
| VSAT | Very Small Aperture Terminal |
| CDF | Cumulative Distribution Function |
| ACM | Adaptive Code Modulation |
| NBN | National Broadband Network |
| FCC | Federal Communication commission |
| RTT | Round Trip Time |
| QoS | Quality of Service |
| ITU | International Telecommunication Union |
| MS | Milliseconds |
| RMSE | Root Mean Square Error |
| SSE | Sum of Squared Errors |
| VS | Versus |
| NTN | Non-Terrestrial Network |

# LIST OF SYMBOLS

| | |
|---|---|
| ***t*** | one-way signal delay (in seconds) |
| ***d*** | distance between the satellite and ground station (in meters) |
| ***c*** | speed of light ($3\times10^8$ m/s) |
| ***f(x)*** | rainfall rate Formula (mm/h) |
| ***x*** | percentage of time exceedance (%) |
| ***a*** | regression coefficient determined through curve fitting |
| ***b*** | regression coefficient determined through curve fitting |
| $\Theta$ | Elevation angle (degrees) |
| ***mm/h*** | Millimeters per hour |
| $R^2$ | Coefficient of determination |
| **P** | Percentile |

# CHAPTER ONE:

# INTRODUCTION

## 1.1 BACKGROUND OF THE STUDY

Over the past decade, High Throughput Satellite (HTS) deployments have increased significantly to support growth of real-time data usage in various sectors in today's world of technologies. This new HTS satellite technology advancement offered higher and more flexible data rates that are crucial in supporting real-time applications such as video streaming, real-time monitoring and big data analytics(Guan et al., 2019). Moreover, it has begun to bridge many unconnected areas, enhancing data throughput and providing larger data set for communication link compared to earlier days. This high throughput data offering has enabled better internet access penetration, leading most telecommunications and internet service providers to expand their coverage globally(Euroconsult, 2022). The rise of HTS also improves real-time remote sensing, which is vital for environmental monitoring and disaster response, while ensuring reliable data transmission for IoT and M2M communication networks(Inigo et al., 2014).

There are a variety of HTS network systems, each with its own unique characteristics and designed to support specific applications. This study focuses on two main satellite orbits, namely Geostationary Earth Orbit (GEO) and Low Earth Orbit (LEO).

GEO satellites are placed in orbits that are approximately 36,000 kilometers (km) above the Earth's surface. These satellites are primarily used for satellite communications and located at fixed positions at Geostationary orbit. They can provide continuous coverage to a specific geographic region. However, because GEO satellites are further away from Earth, they have a longer communication latency (Centenaro et al., 2021).

LEO satellites orbit the Earth at altitudes ranging from 160 to 2,000 km and are currently in trend due to their growing popularity in industries focused on expanding global

internet coverage and providing high-speed connectivity. Due to their closer distance to Earth, LEO satellites offer lower communication latency, which is advantageous for applications that require real-time communication. This has given rise to mega constellations, with SpaceX to possibly deploying 12,000 satellites under its Starlink project. Similar initiatives are being considered by OneWeb and Blue Origin, all with the ambition to offer broadband connectivity on a global scale (Ogutu B. Osoro & Edward J. Oughton, 2021). LEO satellite network systems allow for the utilization of high-frequency bands like Ku, Ka, Q, and V, which offer larger bandwidths compared to those for GEO satellites (Dvořák et al., 2020), thereby enabling higher capacities for users.

Thus, the satellite industry has revolutionized rapidly to fulfill the necessity of high data throughput by launching High Throughput Satellite (HTS) from Geostationary Orbital slot to High Throughput Satellite (HTS) constellations on Low Earth Orbital slot recently (Kodheli et al., 2021).

However, these higher radio frequency bands specifically are going to be impacted during rain where heavy rain can deteriorate the radio frequency signal leading to signal attenuation and weakening it. This occurrence known as rain fade will result in signal impact or degradation of signal quality which finally affecting the communication link performance or total loss in signal during intense rainfall. It is also well known that rain attenuation of radio waves is substantial in satellite communications using frequencies of higher than 10 GHz where all the HTS were built using Ku band (12- 14GHz) and Ka band (20 -40 GHz) (Maekawa et al., 2006). Figures 1.1 and 1.2 illustrate how heavy rainfall can severely affect higher-frequency bands, such as Ku-band and Ka-band, particularly in tropical regions where intense rain is common (Edirisinghe et al., 2023).

Furthermore, demand for satellite communications is rising in South-East Asia, which is one of the heaviest rain regions in the world.(Tech Collective, 2023)There are several studies of comparing rain fade over satellite links especially towards Ku Band ranges from 12-18GHz in tropical area (Maekawa et al., 2006; Mandeep & Hassan, 2006; Pan et al., 2001) but none of these comparing the performance from LEO services within

the tropical region where their services are also operating within the Ku Band frequency range but operating at low earth orbit, nearer to Earth.

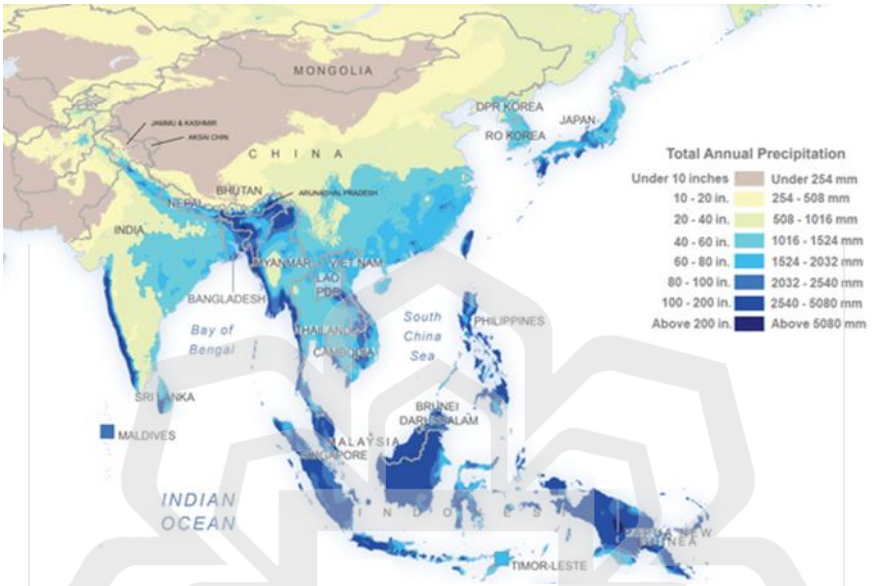



Figure 1.1 East and South Asia Precipitation MAP (United Nations Office for the Coordination of Humanitarian Affairs, 2015)

These overall effects directly influence latency by increasing the time to travel in satellite communication links which refers to the time required for a signal to travel from the ground station to the satellite and back again, completing a full transmission cycle. The greater the distance between the satellite and Earth, the longer this cycle becomes, which results in higher latency. For instance, Geostationary Earth Orbit (GEO) satellites experience longer delays compared to Low Earth Orbit (LEO) satellites because of their higher altitude. In addition, external factors such as rain attenuation can further worsen this condition. Heavy rainfall weakens and slows the signal, forcing retransmissions or additional error correction, which increases the effective Time to Restore (TTR) and consequently, the overall latency of the communication link is impacted.

## 1.2 PROBLEM STATEMENT

Starlink, a Low Earth Orbit (LEO) satellite service introduced in Malaysia in 2023, operates in the Ku- and Ka-bands (12–40 GHz), which are highly vulnerable to rain attenuation. Like GEO HTS, LEO systems also face performance degradation during heavy rainfall(Guan et al., 2019)With Peninsular Malaysia experiencing one of the highest annual rainfalls in Southeast Asia (~2,692 mm), tropical weather conditions present a major challenge to maintain reliable connectivity(Edirisinghe et al., 2023).This raises the critical problem of understanding how rainfall impacts latency in LEO satellites links compared to GEO systems.

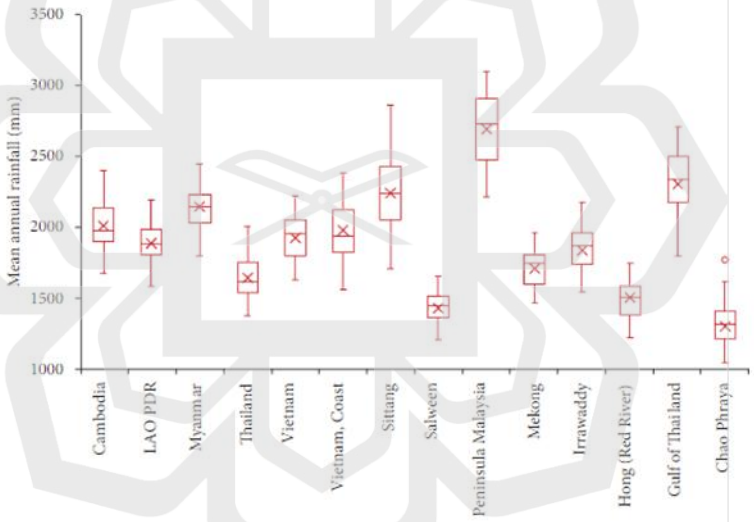



Figure 1.2 Box plot of rainfall distribution of each country(Edirisinghe et al., 2023)

Current analysis on Starlink LEO is widely measuring its capability on application layer with terrestrial and GEO Satellite broadband network. Although Starlink LEO has been shown to perform almost as well as terrestrial networks and better than GEO satellites for applications that are sensitive to delay, there is still very little publicly available data on how it performs under tropical rainfall conditions(Deutschmann et al., 2022).There are many interests from the researcher, public user and subject matter expert exploring data set

from Starlink LEO HTS in comparison towards GEO HTS. At present, no comprehensive study has compared Starlink LEO with GEO HTS in Malaysia, particularly regarding latency effects on link stability, service availability, and the impact of rain attenuation during heavy rainfall. This creates a clear research gap, as rainfall is a major factor affecting satellite signals latency in tropical region. Therefore, a detailed investigation is needed to set up an actual measurement link, analyze it, and correlate the impact of rainfall rate with latency on Starlink LEO with GEO HTS, to evaluate its resilience, reliability, and suitability as an alternative to traditional GEO systems.

## 1.3 PURPOSE OF THE STUDY

The primary goal of this research is to provide a comprehensive **understanding of how rain affects satellite latency in tropical environments** by comparing Starlink LEO with GEO HTS in terms of link stability and availability, and **to develop mathematical correlations of latency in LEO and GEO with rainfall for predicting these effects.** These correlations are essential for designing communication systems that can withstand heavy rainfall and deliver reliable service.

This study is divided into two main categories. The first examines how rain affects Starlink LEO satellite communication latency compared to GEO HTS links in tropical region, where heavy rainfall makes it challenging to maintain stable service availability. Rainfall causes rain attenuation, a phenomenon in which signal strength weakens as it passes through rain. The second focuses on analyzing the correlation rain-induced latency by comparing Low Earth Orbit (LEO) constellations with Geostationary (GEO) satellite communication links in tropical environments.

### 1.3.1 Focus on Two Satellite Systems

This study compares two types of satellite systems commonly used for communication:

Table 1.1 LEO Satellite specifications

| | |
|---|---|
| **Low Earth Orbit (LEO)** | Altitude at 500 to 2,000 km |
| | Requires multiple satellites for big coverage areas |
| | Stronger signals, **lower latency**, high data throughput |
| | Less affected by rain due to proximity to Earth |

Table 1.2 GEO HTS Satellite specifications

| | |
|---|---|
| **Geostationary Earth Orbit (GEO) HTS** | Altitude: 36,000 km |
| | Single, Fixed location, covers large areas |
| | **Higher Latency**, variable (low to high) data throughput |
| | Highly affected by rain and highly impact when it happens due to longer distance |

### 1.3.2 Challenges in Tropical Regions

Tropical areas are characterized by frequent and intense rainfall, high humidity, and dense cloud cover. These factors make tropical regions particularly challenging for satellite communication. Rain attenuation is especially severe in these environments:

Table 1.3 Challenges for Rain-induced Latency impacting Satellite link

| Challenges | Description |
|---|---|
| **High Rainfall Intensity** | Tropical storms and monsoons produce heavy rainfall that weakens satellite signals significantly. |
| **Raindrop Size Distribution** | Larger and varied raindrop sizes scatter and absorb electromagnetic signals, increasing attenuation. |
| **Frequent Storm Events** | Persistent and recurring storms in tropical regions raise the likelihood of frequent signal disruptions. |

Understanding these unique challenges is critical for developing effective communication systems in tropical areas, where reliable connectivity is essential for economic growth, disaster response, and social development.

## 1.4 RESEARCH OBJECTIVES

The objective of this research is to perform a comparative study and provide refined communication link improvement in term of latency effects on its physical communication link for low earth orbit HTS mega-constellations satellite against a single HTS geostationary satellite in the tropical region.

First Objective:

- To establish a comparative latency measurement framework for GEO HTS and LEO satellite networks for comparative performance evaluation.

Second Objective:

- To assess the latency performance of Starlink LEO and SES 12 (GEO HTS) satellite communications under tropical rainfall conditions using empirical measurement data.

Third Objective:

- To develop rain-induced latency correlation models for Starlink LEO and SES-12 GEO High Throughput Satellite (HTS) systems using empirical measurement data collected under tropical rainfall conditions.

## 1.5 RESEARCH SCOPE

This research aims to analyze the effects of latency on satellite communication links operating in the Ku Band specifically focusing on Starlink LEO constellations and SES-12 GEO HTS systems within tropical atmospheric regions like Malaysia. The primary goal is to have predictable latency correlation vs rainfall rate for tropical environments by using empirical rainfall data and actual satellite link measurements.

This study is limited to the analysis of latency effects on Starlink LEO and SES-12 GEO HTS systems within tropical regions. It does not cover Medium Earth Orbit (MEO) satellites, the design and implementation of satellite terminals or ground infrastructure, or the evaluation of adaptive mitigation techniques such as power control and adaptive coding and modulation (ACM). Additionally, the performance of satellite communication systems outside tropical climates and global assessments of Starlink's network are beyond the scope of this research.

# CHAPTER TWO

# LITERATURE REVIEW

## 2.1 OVERVIEW

Chapter Two introduces the relevant theoretical backgrounds which are considered essential for this research. This chapter explores the key principles and existing studies related to satellite communication systems, latency impact and the unique environmental challenges posed by tropical regions for satellite communication.

## 2.2 HTS SATELLITE SYSTEM OVERVIEW

An HTS is a type of satellite designed to handle a large volume of data communication link, offering high data throughput capabilities. These satellites are equipped with advanced technologies such small spot beam in large numbers being deployed and distributed over a particular service area to support high-speed data communication, broadband services, and other data-intensive applications. HTS combine a unique spectrum efficiency and performance of spot-beam antenna with ultra-wideband transponder to enable higher level of data link throughput. Each spot beam reuses back the frequencies in multiple transponders or carrier which single HTS can provide more than 100Gbps of capacity this is more than 100 times the capacity offered by conventional Ku Band satellites(Vidal et al., 2015)

The first HTS, Thaicom-4 known as IPSTAR was launched in 2005 by Thaicom Public Company Limited with a global capacity of 45 Gbps. This was followed by the launch of ViaSat-2 in 2017, offering over 300 Gbps of capacity (Geng et al., 2019). After the period of 2005–2017, the yearly launch rate of HTS has increased tenfold with a single HTS can provide much as throughput as the entire traditional wide-beam communication satellites in Geostationary Orbit (Geng et al., 2019). Indirectly this massive increase in

bandwidth, the affordability of the bits per second or cost of throughput with HTS is getting lower comparing to conventional wide-beam satellites by one or two orders of magnitude and it is reaching terrestrial-like economics (Guan et al., 2019).

### 2.2.1 HTS in Geostationary Orbit

A geostationary orbit is a specific type of orbit where a satellite orbits the Earth at the same rate as the Earth's rotation. A geostationary satellite (GEO) is an earth orbiting satellite located at an altitude of approximately 36,000 km from earth. This shows that the satellite appears stationary to a fixed point on the Earth's surface (Geng et al., 2019). Geostationary orbital slots are specific positions in geostationary orbit where satellites are stationed to provide coverage over designated regions where these slots are allocated by international regulatory bodies to prevent interference between satellites. Positioning an HTS in a geostationary orbital slot allowing the satellite to provide high speed data services over a specific geographic area and due its stability in fixed location, its offer reliable and consistence high data throughput for the communication link by adopting wide bandwidth or higher frequency i.e. Ku/Ka Band. HTS in geostationary orbital slot are commonly used for broadband internet services, mobile communications, video streaming and private data transmission for remote location to centralized data storage (Christopher McLain & Janet King, 2017). However, since geostationary satellites have lifetimes of up to 15 years, traffic demands, service areas, and applications often change rapidly during this period (Hobbs et al., 2015).

In Southeast Asia, the HTS market was initially dominated by Thaicom-4 (IPSTAR). For example, Australia's National Broadband Network (NBN) launched its Interim Satellite Service (ISS) in July 2011 by leasing IPSTAR capacity to provide broadband for rural and remote areas (NBN Co, 2017). However, as a large number of regional and international players are incorporating HTS into their fleets, the current landscape is changing quite rapidly (Shagun Sachdeva, 2018). SES a global satellite operator based in Luxembourg has expanded its capabilities to provide it services via SES-

12 High Throughput Satellite (HTS) expanding for data connectivity services in the Asia-Pacific region starting 2018 (SES, 2019).

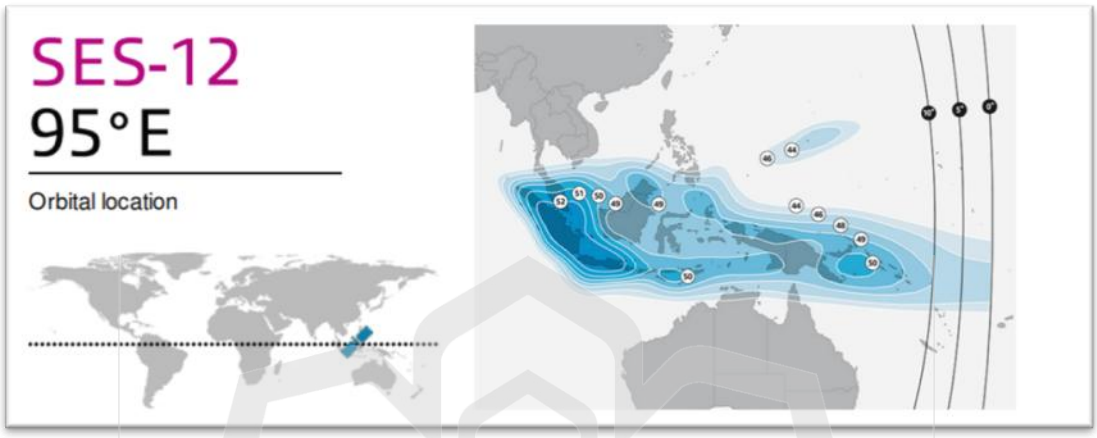



Figure 2.1 SES-12 satellite with malaysia footprints (SES S.A., 2025)

### 2.2.2 HTS in Low Earth Orbit(LEO)

In April 2019, there were two announcements were made that Amazon Inc. is planning to develop a High Throughput Satellite (HTS) constellation for broadband services with over 3,000 satellites in Low Earth Orbit (LEO) known as Project Kuiper and SpaceX obtained approval from Federal Communication commission (FCC) to launch nearly 1,6000 satellites in its LEO HTS constellation known as Project Starlink(Jason Rainbow, 2023). Project Starlink has shown a novel approach in HTS compare to HTS in a traditional GEO network as illustrated in Figure 2.1, which shows its globally expanding coverage. Project Starlink introduced innovation and technology to the recent GEO HTS network. This novel LEO network has the potential to improve overall communication services by reducing satellite latency, increasing bandwidth, and disrupting traditional GEO-based satellite service. From an economic perspective, LEO HTS constellation offers greater scalability than other systems in terms of capacity augmentation. This is because a constellation can be effortlessly expanded without causing any interruption to the existing broadband

services (Ogutu B. Osoro & Edward J. Oughton, 2021). Placing an HTS in LEO offers advantages such as lower latency, reduced signal propagation loss, and increased data transmission speeds due to the satellite's proximity to Earth. Another significant benefit of LEO systems is their ability to serve remote areas, supported by their mobility and the ease of installing user terminals, which are much smaller compared to GEO terminals(Agnelli et al., 2014). This is especially useful in areas with extreme terrain, such as cliffs, valleys, steep slopes, or disaster-prone regions, where building terrestrial networks is often too costly and complex.

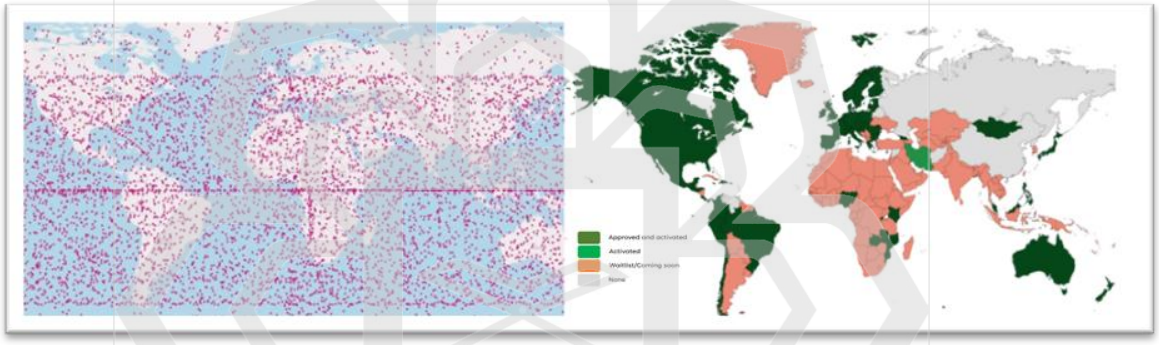


Figure 2.2 Starlink satellites and footprints

Table 2.1 Comparison between SES12 and Starlink specifications

| Satellite Name | Type | Frequency band | Satellite Count | Lifespan | Nominal Latency | Data Throughput |
|---|---|---|---|---|---|---|
| SES12 | Geostationary (GEO) HTS - Specific wide beam covers the entire Asia-Pacific region | Ku-band (VSAT Terminal) & Ka- Band (Gateway) | 1 | 15 years | 500-700 ms | Download of 50-100Mbps & Upload of 10-20 Mbps |

| Satellite Name | Type | Frequency band | Satellite Count | Lifespan | Nominal Latency | Data Throughput |
|---|---|---|---|---|---|---|
| Starlink | Low Earth Orbit (LEO) mega constellation - Global coverage with focus on underserved and remote areas. | Ku-band (Starlink Terminal) & Ka- Band (Gateway) | > 3000 | 5 to 7 years | 20-40 ms | Download of 100-250 Mbps & UL of 20-40 Mbps |

## 2.3 RAINFALL EFFECT IN SATELLITE COMMUNICATION LINK

### 2.3.1 Rain Type and its Effect in Tropical Regions

Rainfall plays a significant role in satellite communication because it can attenuate electromagnetic signals and increase communication latency. From the perspective of wave propagation, rainfall is typically classified into two main types, which are stratiform rain and convective rain. Understanding these types is essential because they directly influence the reliability, signal strength, and latency of satellite links, particularly in tropical regions where heavy rainfall is frequent. Stratiform rain, produced by stratus clouds, is generally light with limited vertical extent but covers a wide area, causing relatively moderate signal attenuation. In contrast, convective rain, produced by cumulus clouds, is more intense with greater vertical extent over smaller areas, leading to stronger signal attenuation and posing greater challenges for satellite communications (Powell et al., 2016). Convective rain is the major cause of communication link outages in the tropic regions and Southeast Asia region (Han et al., 2021). Stratiform and convective rain can be distinguished by their rainfall rates. In this region, stratiform rain is usually below 10 mm/h, while convective rain is

typically above 10 mm/h (Ahmad et al., 2024).

Rainfall rates in tropic regions vary widely across different geographical areas. It is therefore important to study rainfall characteristics based on local conditions. Malaysia is unique in this regard, as it experiences an equatorial climate influenced by tropical monsoons. Malaysia experiences very high rainfall rates that can exceed 200 mm/hour, driven by its tropics climate combined with seasonal monsoon and frequent thunderstorms. These climatic conditions often produce intense, short-duration downpours, especially during the inter-monsoon periods, making Malaysia one of the wettest countries in Southeast Asia (Nor Hisham Haji Khamis, 2005).

### 2.3.2 Rain Attenuation for Satellite Communication Link

Propagation is the way where radio signals are transmitted from one point to another inside the earth's atmosphere over space. Since these are electromagnetic waves, it exhibits properties such as reflection, refraction, diffraction, absorption, polarization and scattering (Ajayi Taiwo Seun, 2007).

There are many effects consideration during designing earth-space link communication link. Any satellite link services, either its HTS or Non-HTS residing in any orbits are open to the effects of the non-ionized atmosphere and the impact becomes stronger if the frequencies are above 10GHz. Technically the effects included absorption in atmospheric gases absorption, scattering and depolarization by hydrometeors. ("ITU-R P618.14," 2023).

Atmospheric losses occur in the earth's atmosphere as a result of energy absorption by the many atmospheric conditions which one of them from bad weather condition. Weather related losses such as rain in this analysis are referred to as atmospheric attenuation and absorption losses. Indirectly, satellite signal link performances operating beyond 10GHz are exposed to propagation loss, where rain attenuation is highly unpredictable

depending on the liquid water content which will impose a major impact on signal link attenuation("ITU-R P.839-4," 2013).

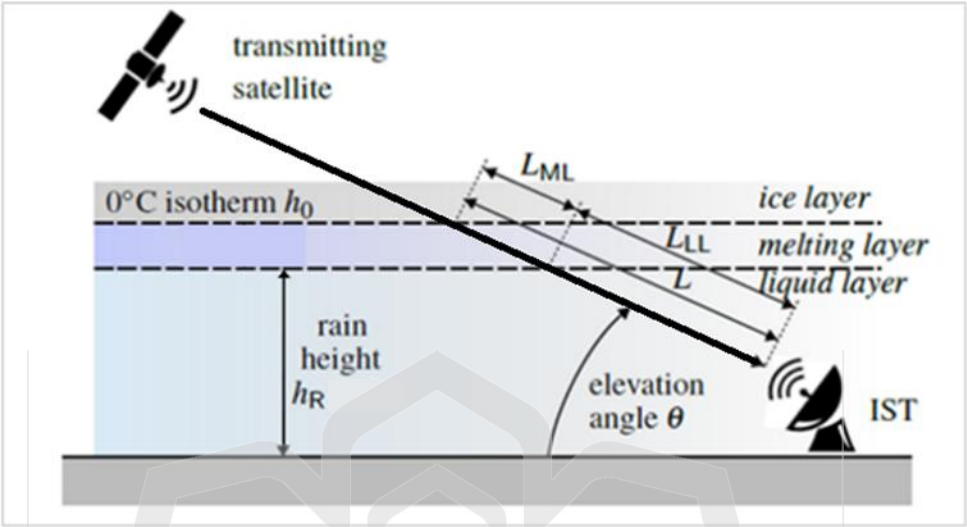



Figure 2.3 Satellite communication link propagation loss (Usha* & Karunakar, 2020)

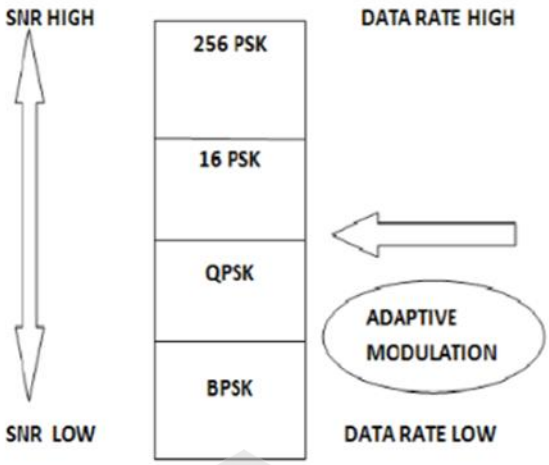
In tropical regions, rain attenuation is considered one of the dominant contributors to propagation loss for any satellite operating frequencies above 10GHz. This propagation effect causes the received signal at remote terminal to be attenuated causing the satellite earth station or VSAT remotely will suffer outages during rain (Mandeep & Hassan, 2006). Annual precipitation data shows Peninsular Malaysia experiences the highest average annual rainfall compared to the neighboring country within the Asia Pacific region (Edirisinghe et al., 2023).

Since then, rain attenuation models have been used to estimate how much the signal is weakened when passing through rain. Starlink elevation is found to be between 15 and 35° but this finding is for temperate or higher-latitude countries. The equatorial region's elevation angle of Starlink has not yet been identified. No simplified calculation method can be determined for LEO systems, the variation in elevation angle must be included in the calculations(Gongora-Torres et al., 2023)

### 2.3.3 ACM Introduce to Reduce Attenuation but not Latency Impact

Although satellite equipment is designed to transmit at high power to support higher modulation schemes and greater data throughput, it remains sensitive to signal losses. Maintaining higher modulation in satellite communication during rain is a challenge due to the phenomenon known as rain fade, where heavy rain will attenuate its signal. Rain fade directly reduces the signal-to-noise ratio (SNR), which is critical for sustaining advanced modulation techniques, but simple adaptive code and modulation (ACM) adaptation methods can effectively mitigate these effects and maintain target packet-error rates even under severe signal fading(Bischl et al., 2010). This digital modulation technique requires more complex and expensive hardware and software, and more power to maintain a given SNR (Rajat Acharya, 2017) Furthermore, satellite communication standards are designed to cope with severe fading phenomena and long propagation delays characterizing the satellite channel. Therefore, implementing ACM to dynamically switch to lower-order modulation schemes during adverse conditions, maintaining link reliability at the cost of reduced throughput.

The benefit of these digital modulation schemes is to reduce the bit error rate (BER) and increase the SNR of the signal, by allowing the receiver to detect, correct errors and select the best transmission mode to be used which in this case interrupted by rain(Skarzynski et al., 2016). Figure 2.4 shows coding schemes also enable the use of adaptive coding and modulation (ACM), where the modulation and coding parameters are adjusted automatically according to the channel conditions, to optimize the throughput and quality of service (QoS)(Rinaldo et al., 2004)




| Mode No. | Modulation /code rate | SNR range [dB] | Rb [bit/symbol] |
|---|---|---|---|
| 1 | BPSK 1/2 | 6-10 | 0.5 |
| 2 | BPSK 2/3 | 8-12 | 0.67 |
| 3 | QPSK 1/2 | 10-14 | 1 |
| 4 | QPSK 2/3 | 12-16 | 1.33 |
| 5 | 8-PSK 1/2 | 14-18 | 1.5 |
| 6 | 16-APSK 1/2 | 16-20 | 2 |
| 7 | 16-APSK 2/3 | 18-22 | 2.67 |
| 8 | 16-APSK 3/4 | 20-24 | 3 |
| 9 | 16-APSK 5/6 | 22-26 | 3.33 |
| 10 | 16-APSK 7/8 | 24- | 3.5 |

Figure 2.4 Modulation technique flow versus SNR (Jaya et al., 2016)

## 2.4 LATENCY IN SATELLITE SERVICES

In research papers, satellite latency is best captured by defining the measurement methods, considering different orbital heights and acknowledging the impact of data transmission and processing delays. Specifically, research should be able to differentiate between round-trip time (RTT), which is the time it takes for a packet to travel to the satellite and back, and other forms of delay like processing time on the satellite(Reyouchi et al., 2017). Low Earth orbit (LEO) satellites operate at altitudes of approximately 180–2,000 km above the Earth's surface, which is significantly lower than geostationary (GEO) satellites orbiting at

about 36,000 km. This shorter distance enables much lower latency and higher data throughput for space–ground communication(Ma et al., 2023). Measurement methods can be described below.

### 2.4.1 Latency Known as Round-Trip Time (RTT)

Round trip times can be measured by using a simple tool such as ping, which is available as a command or as part of an app on most systems today(Truman et al., 2002).Measurement methods for latency described in section 2.4.1.1 and 2.4.1.2. This is a fundamental measure of latency and involves sending a packet and measuring the time it takes for response to return.

#### *2.4.1.1 Data Transmission and Processing Delay*

This refers to the time it takes to transmit data from the satellite to the ground station including the time the satellite spends processing the data before transmitting it. Delays within a communication network can arise from various sources, including signal propagation, queuing, processing, and transmission(Heine et al., 2024).

#### *2.4.1.2 Experimentally Measured Latency*

For the most accurate portrayal, research should include experimental data collected using real-world satellite networks. In satellite communication systems, signal delay is an important performance factor. The delay can be calculated using the following formula:

$$t = \frac{d}{c} \tag{2.1}$$

where:

t = one-way signal delay (in seconds),

d = distance between the satellite and ground station (in meters),

c = speed of light ($3\times10^8$ m/s)

For a full round-trip time (RTT), the delay is doubled:

$$RTT = 2\ x\ t \quad (2.2)$$

Low Earth Orbit (LEO) satellites, operating between 500 and 2,000 km above Earth, typically achieve ideal RTTs of 3 to 10 milliseconds. However, in practice, LEO networks show RTTs average 50 milliseconds due to additional routing and processing delays(Donal McCarthy, 2022). Geostationary Earth Orbit (GEO) satellites, located at an altitude of 36,000 km, have a theoretical RTT of around 238 milliseconds. In real-world conditions, GEO satellite RTTs are often between 500 and 600 milliseconds.

### 2.4.2 Latency Impacting on Satellite Link Performance

Rainfall can significantly impact satellite link performance, particularly in the Ku- and Ka-band frequencies. The primary effect is rain attenuation, which reduces signal-to-noise ratio (SNR) and can trigger adaptive coding and modulation (ACM) changes, retransmissions, and queuing delays(Claypool et al., 2021). This can increase end-to-end latency, depending on the system design. Latency in satellite communications mainly comes from the time it takes for signals to travel between the Earth and the satellite, along with extra delays from processing and queuing at ground stations, gateways, and user terminals. Average latency values mean or median give a general idea of performance, but it does not show the full picture. For real time services or applications, sudden spikes in delays, even though rarely happen, can seriously reduce the quality of service.

#### *2.4.2.1 Latency Tail in Satellite Services*

To better capture performance variability in satellite communications, it is important to look beyond average delay. In GEO satellite systems, the average round trip latency is already high averaging at 600 ms, and the latency tail extends further under conditions such

as rain fade in this scenario sometimes pushing beyond 1 second(Maral et al., 2020). This makes interactive applications like video conferencing or gaming nearly unusable during tail events (Van Damme et al., 2024). In LEO constellations, the average latency is much lower averaging in between 30–50 ms, but latency tail events still occur. These are often linked to handovers between satellites, dynamic routing, or rain fade, causing spikes in delay well above the mean. Even though the average is low, these rare delays can disrupt real-time services, making the latency tail as important as the mean in performance evaluation (Sriraman et al., 2017). In evaluating real user experience, satellite network studies often report not only mean latency but also high-percentile delays (e.g., P95, P99), since these extreme cases can degrade interactivity, responsiveness, and user satisfaction (Dean & Barroso, 2013). The latency tail of this distribution refers to the higher percentile values which are typically measured at P95, P99 or even P99.95. This situation captured the worst delays experienced by a small fraction of packets. For example, while 99% of packets may arrive within the $99^{th}$ percentile threshold, the remaining 1% may face significantly higher delays. Such latency tail events in satellites can result from rain fade in Ku/Ka-band links, which triggers adaptive modulation, retransmissions, or queuing from gateway congestion or beam hopping, which introduces variable queuing times. Although these events are relatively rare, they are crucial for user perceived quality. Real-time applications like video conferencing, online gaming, and cloud services are highly sensitive to sudden spikes in delay, meaning that even if the average latency is low, poor tail performance can make the service feel unresponsive. A percentile represents the latency value below which a specified percentage of packets is observed. For this reason, latency tail is now recognized as a key performance metric where the P99 response time rather than the average often determines user satisfaction and system robustness(Dean & Barroso, 2013).

Latency distributions sampling in Figure 2.5 illustrated using Cumulative Distribution Function (CDF) plots, where the latency tail is visible at higher percentile of P95 -P99. Such plots clearly show how a small fraction of packets experience disproportionately high delays.

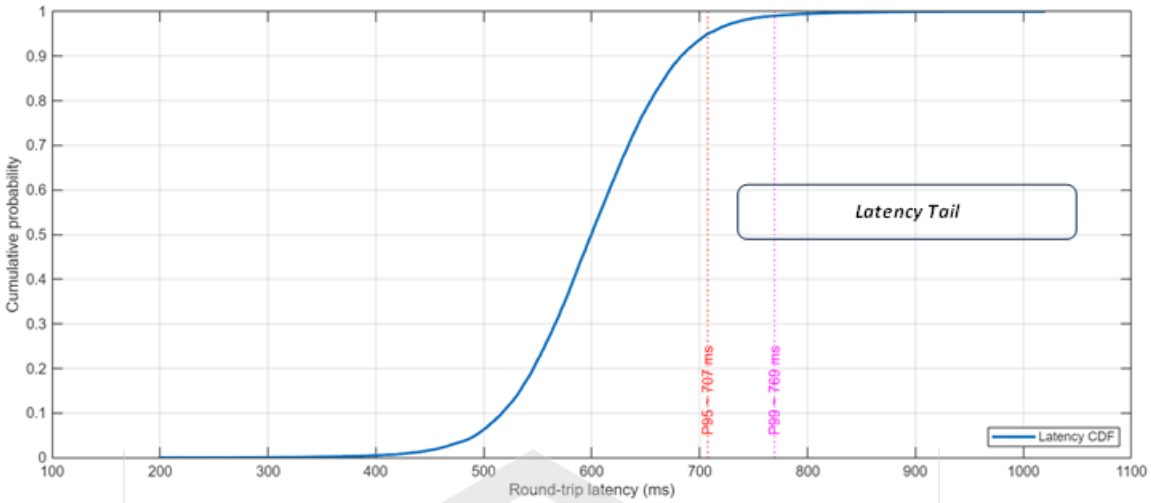



Figure 2.5 CDF of GEO Satellite with latency tail

The latency performance of LEO and GEO satellite systems differs significantly in tropical regions, where heavy rainfall frequently causes severe signal degradation in Ku-band links. LEO constellations such as Starlink are able to mitigate these effects from its height with multi-satellite handovers, whereas GEO satellites are more susceptible to prolonged attenuation and service disruption. Rain-induced degradation further increases the latency fluctuations. However, no established correlation between rainfall rate and latency or round-trip time (RTT) in tropical regions has been reported to date.

Table 2.2 Satellite Latency and Distance Comparison GEO, MEO and LEO

| **Satellite Type** | **LEO** | **MEO** | **GEO** |
|---|---|---|---|
| Satellite Height (km) | 500-1500 | 5000-12000 | 36000 |
| Orbital period | 95-115 min | 3-7 hours | 24 hours |
| # of satellites, coverage | 40-800 Global | 8-20 Global | 3 (no polar coverage) |
| Satellite life (years) | 3-7 | 10-15 | 15+ |
| handoff Frequency | High | Low | None |
| Gateway Cost | Very Expensive | Expensive | Cheap |

| | | | |
|---|---|---|---|
| Doopler | High | Medium | Low |
| Round-trip propagation delay | 10-30 ms | 70-200 ms | 0.5s |
| Propagation path loss | Least | High | Highest |

Table 2.3 Summary of literature review

| **Author** | **Title** | **Research Focus** | **Finding** | **Limitation** |
|---|---|---|---|---|
| Kunadi et al. (2024) | An Efficient Predictive Handover in LEO Satellite Networks using LSTM — IEEE COMNETSAT 2024 Systems (2022) | LEO Rain attenuation model using prediction variable elevation angle | Explains how predictive handovers help maintain low LEO latency under mobility. | On simulation data, no rain or real-time hardware effects. |
| Schroder et al. (2025) | A Performance Study on LEO Satellite Networks with ISLs — IEEE SysCon 2025 | Impact of inter-satellite link topology on LEO latency and stability. | Provides architectural context for interpreting LEO latency paths. | Idealized propagation, no weather or processing latency delays. |
| Yusoff et al. (2024) | A Study on Latency in L-Band LEO Satellite Networks for IoT Applications — IEEE APACE 2024 | End-to-end latency in L-band LEO IoT networks. | Provides real-world baseline latency measurements for LEO systems. | L-band IoT only, no weather and latency measurement. |

| Author | Title | Research Focus | Finding | Limitation |
|---|---|---|---|---|
| Kim et al. (2022) | Analysis of Low-Latency Virtual Network Resource Reservation for LEO Satellite Network — IEEE APCC 2022 | Simulation-based analysis of slicing under satellite mobility. | Physical testbed measuring gateway-to-cloud latency under different terminal placements. | Stable average latency is based on simulation only. |
| Osoro & Suki (2020) | An Evaluation of Link Performance Based on Rainfall Attenuation for a LEO Communication Satellite Constellation Over Africa — IEEE | Rain attenuation impact on Ka-band LEO uplinks in tropical regions. | ITU-R models overestimate rain attenuation; low-rain regions perform best. | Rain effects only, no real-time latency measurements |

## 2.5 SUMMARY

The summary of the literature review on communication link performance for geostationary (GEO) satellites versus low Earth orbit (LEO) satellite networks in tropical regions presents the findings and significant limitations from past studies, as outlined in table 2.3. The literature review revealed a significant lack of empirical data on the relationship between latency and rainfall rate for Starlink LEO systems in tropical regions, highlighting the novelty and contribution of this study to the field of rain-induced satellite latency analysis. Despite the increasing deployment and usage of Starlink services worldwide, there is a noticeable lack of comprehensive studies and empirical data that evaluates its effectiveness and reliability under the specific environmental conditions prevalent in tropical weather.

# CHAPTER THREE

# METHODOLOGY

## 3.1 OVERVIEW

This chapter presents the research methodology adopted in this study. An empirical and evidence-based approach was employed to ensure reliable and reproducible results. The methodology is organized into three main phases: (1) a comprehensive study was undertaken to evaluate satellite communication performance metrics, assess latency under tropical rainfall conditions, compare findings with ITU-R rainfall rate models, and select the most suitable GEO and LEO terminals for implementation in a real test environment; (2) a systematic evaluation of satellite latency monitoring approaches was performed to establish an automated and synchronized data acquisition framework, including the assessment of monitoring tools and data collection techniques to ensure accurate, reliable, and continuous latency measurements throughout the study; (3) followed by comparative analysis, deriving link availability and come out with latency rain-induced correlation to achieve research objectives.

## 3.2 SATELLITE TECHNOLOGY IN TROPICS CLIMATE

The first phase involves studying satellite technology developments by reviewing past research papers related to rain attenuation in Ku-Band satellite communication links, identifying the necessary onsite equipment and available satellite services operated in the region as part of high-level planning, developing framework, and understanding the impact of rain attenuation using rainfall rate references provided by ITU-R P618.14 (2023), which offers guidelines for calculating rain effects on satellite signals at frequencies up to 55 GHz.

Subsequently, next focus of this research is to evaluate the impact of rain fade on the latency of Ku-band Geostationary Earth Orbit (GEO) High Throughput Satellites (HTS)

and Low Earth Orbit (LEO) Satellite Network communication links operating in Malaysia systematically, a country located within the tropical region. This study aims to analyze the degradation of latency signals due to rain attenuation, assess its effects on the performance of both GEO and LEO satellite systems, and compare the behavior of these systems under varying rainfall intensities specific to tropical climates. The results of this evaluation will provide valuable insights into the operational limitations and performance optimization of satellite communication systems in regions prone to heavy precipitation.

### 3.3 ONSITE MEASUREMENT AND DATA COLLECTION

LEO Starlink and SES-12 GEO HTS VSAT terminals are co-located and were installed at satellite communication lab at the International Islamic University Malaysia (IIUM). This phase comprises setting up and testing satellite link services using Ku Band transmission from two different satellite systems, which is LEO Starlink and conventional SES-12 GEO HTS, a Geostationary Earth Orbit (GEO) satellite. A real-time gravity tipping bucket rain gauge is integrated into this setup to measure rainfall intensity accurately. It records data at one-minute intervals, providing high temporal resolution for detailed analysis. With a measurement resolution of 0.28 mm, the system ensures precise detection of even light rainfall events. Subsequently, satellite link latency was captured at 10 ms intervals and monitored continuously through a customized command prompt as shown in Figure 3.4 serving as a primary parameter for understanding the behaviour of satellite communication links under tropical weather conditions. By implementing this automated monitoring approach, the methodology provides a comprehensive dataset for further analysis.

LEO Starlink terminal is connected via LEO Starlink Satellite network, as shown in Figure 2.2, which is marked as an approved and activated region on the map. This LEO Starlink terminal is physically set up on a pole using a custom extended mount shown in Figure 3.1 and performs an automatic alignment to locate and connect with Starlink satellites. The terminal will connect to the Starlink network and provide internet access.

The Starlink terminal stays in a fixed position while tracking Starlink satellites using its advanced flat panel phased array antenna as shown in Figure 3.1. Utilising a phased array antenna for electronically steered beam control, the Starlink terminal tracks satellites by its integrated a GPS receiver for its location with Starlink satellites' ephemeris data to predict satellite positions. Compared to a VSAT parabolic antenna, a phased array antenna scans faster due to electronic beam steering, while the parabolic antenna depends on the initial mechanical setup of its azimuth and elevation(Ma et al., 2023).

However, for the Starlink terminal, information regarding its azimuth and elevation angles is not publicly available through its standard product dashboard. Therefore, the Starlink azimuth and elevation angles are obtained separately using the open-source Starlink-Grafana-Dashboard tool, which was developed through outsourced scripting (Stephen Shamakian, 2021). This tool was specifically created to capture the Starlink terminal's azimuth and elevation angles and to enable continuous monitoring of these parameters. Based on this setup for 6 months of observation, the azimuth and elevation angles measured in Kuala Lumpur, Malaysia, are approximately 4° and 76.5°, respectively.

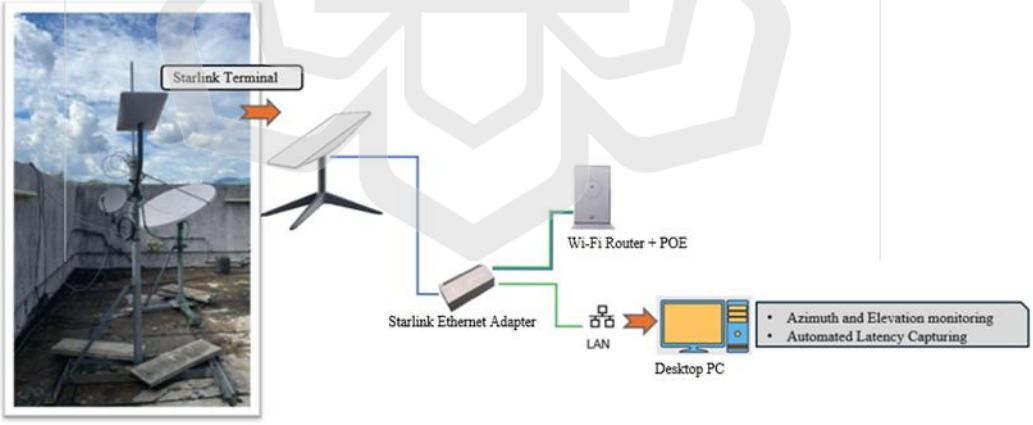



Figure 3.1 Onsite experimental arrangement for Starlink

Figure 3.2 shows the SES-12 GEO HTS Ku-band terminal setup. The VSAT terminal is connected to the SES-12 Satellite, which is positioned in a Geostationary orbit at 95° East with a fixed azimuth of 244.35° and elevation of 81.20°(SES S.A., 2025).

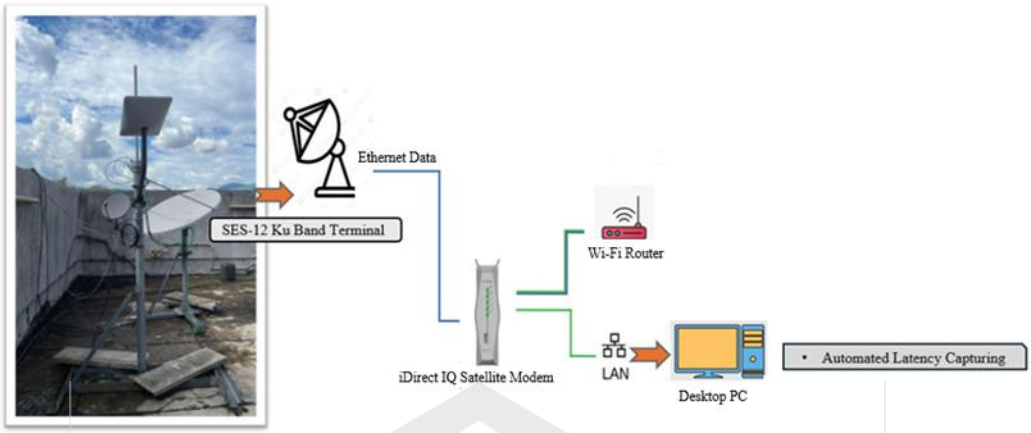



Figure 3.1 Onsite experimental arrangement for SES-12 GEO HTS

This orbital slot shown in Fig. 2.1 allows SES-12 GEO HTS to provide coverage across the Asia-Pacific specifically covering the Malaysia region in providing a range of communication services.

A batch script was developed during this stage to automate the measurement of satellite link latency. The script was developed specifically for this assesment to ensure continuous operation, logging real-time data by sending ping requests to Google's DNS server (8.8.8.8) for both satellite links (SES-12 GEO HTS and LEO Starlink). An automated script as shown in Figure 3.3 runs continuously, measuring and recording latency results for every 10 seconds. These results are saved in a file named ping_log.txt and are also displayed in real-time on the desktop PC, allowing users to monitor the data as it updates. Figure 3.4 shows a simplified block diagram of the automated script process, where results are stored in Google Cloud Storage in a structured format for future analysis.

```
@echo off
setlocal enabledelayedexpansion

if not exist ping_log.txt echo Date,Time,Reply > ping_log.txt
:loop
set timestamp=%date% %time%
ping 8.8.8.8 -n 1 > temp_ping.txt
set response=

for /f "delims=" %%A in (temp_ping.txt) do (
    set line=%%A
    if "!line:~0,1!"=="R" (
        set response=!line!
    )
)

echo %timestamp%, %response% >> ping_log.txt
type temp_ping.txt
timeout /t 10
goto loop
```

Figure 3.3 Customized command for automated latency capturing

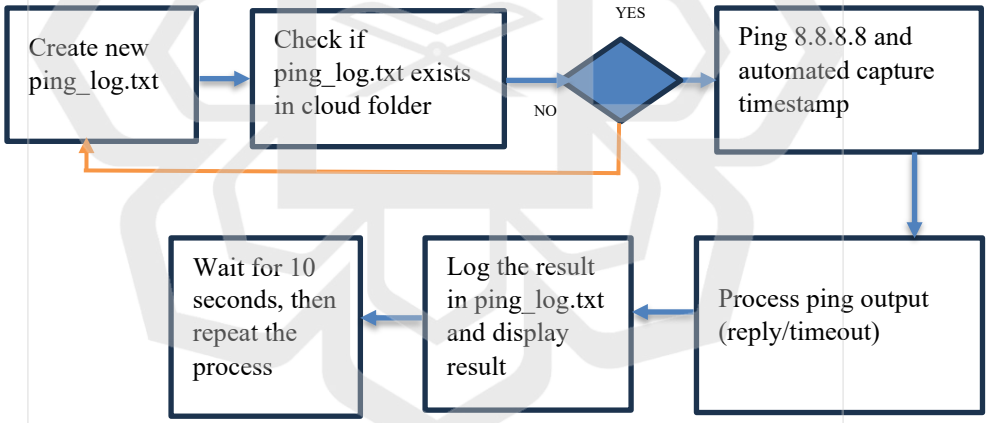



Figure 3.4 Flow Chart for Automated Latency Script

## 3.4 LATENCY TAIL ANALYSIS

### 3.4.1 Latency Tail Interpretation

The percentile latency values indicate the latency limits experienced by most packets. For example, the 99th percentile latency means that 99% of packets experience a lower latency

than this value, while only 1% experience higher latency. The difference between the average and the high-percentile values shows the severity of the tail. For instance, in a GEO satellite link the average latency is typically around 600 ms, but the 99% latency can sometimes reach 900 ms or more. This indicates that although most packets fall close to the mean, a small fraction of packets are delayed much longer.

These tail delays are usually linked to specific conditions. Longer propagation paths at low elevation angles can increase transmission time. Atmospheric impairments such as rain fade in Ku- and Ka-band systems may force the system to use adaptive modulation and coding (Sonata et al., 2020), which in turn leads to retransmissions or buffering. In LEO constellations, switching between satellites during handover can temporarily push delays far beyond the average.

Understanding these causes is important because user experience is heavily affected by such tail events. Real-time applications such as video conferencing, cloud access, or gaming may appear to freeze or respond very slowly during these rare but severe delays, even if the overall average performance looks acceptable.

### 3.4.2 Latency Tail Visualization

To make tail latency easier to understand, latency distributions are often illustrated using Cumulative Distribution Function (CDF) plots. A CDF shows the proportion of packets that arrive within a given delay threshold. On the x-axis, latency values are displayed, while the y-axis shows the cumulative probability. By marking key points such as the 50th percentile (50%), 95th percentile (95%), and 99th percentile (99%), the “tail” of the distribution becomes visible on the right-hand side of the curve.

These plots are useful because they clearly show how a small percentage of packets experience much higher delays than the majority. In the case of GEO satellites, the entire

distribution is shifted to higher values, with a long and predictable tail extending further right. For LEO satellites, the main distribution is concentrated at much lower values, but occasional spikes caused by handovers or congestion can still be observed in the tail. Including such graphs in the thesis provides readers with a visual representation of latency behavior and highlights why average values alone are not sufficient to describe performance.

### 3.4.3 Latency Tail Interpretation and Implications

Finally, the results of the tail analysis and the CDF plots should be interpreted in the context of user experience and system design. From the user's perspective, even if 99% of packets meet acceptable thresholds, the small percentage of tail events can still cause noticeable disruptions. For GEO systems, this explains why they are not well suited for applications that require real-time interaction, since their already high average latency can become unusable during tail events that exceed one second. For LEO systems, the averages are much lower, but the tail still reveals moments of poor performance during handovers or periods of congestion.

Therefore, reporting and analysing tail latency is essential for ensuring that performance assessments reflect the actual quality of experience for end users.

## 3.5 CURVE FITTING SCENARIO AND CORRELATION

The purpose of the curve fitting process was to establish mathematical correlation that describe how rainfall rate and satellite latency behave under different operational and environmental conditions. Since both parameters exhibit nonlinear characteristics, especially under heavy rain, nonlinear regression was employed to obtain best-fit functions that could predict latency behavior as a function of rainfall intensity.

The collected six-month measurement dataset, an initial statistical examination was

first performed to assess the behaviour of rainfall rate and latency with respect to time-exceedance probability. The preliminary analysis showed that neither parameter follows a linear relationship. To establish an appropriate correlation between rainfall rate and latency, a model-selection procedure was adopted. Rainfall rate and latency data were first paired using a common time-exceedance framework to ensure consistent statistical representation. Non-linear functional forms were considered as candidate models to describe the rainfall–latency relationship.

To accurately capture these dynamics, curve fitting was applied using MATLAB's Curve Fitting Toolbox. This method allows the conversion of large, discrete datasets into continuous, analytical expressions, which can then be used to quantify the degree of correlation between rainfall rate and latency and to identify threshold regions where nominal performance transitions into nominal or tail latency categories. The relationships were analyzed using MATLAB's Curve Fitting Toolbox. The rainfall rate vs. time exceedance followed a logarithmic correlation:

$$R = a \log(x) + b \tag{3.1}$$

The latency vs. rainfall rate relationships exhibited power law behavior, depending on whether the region represented nominal or tail conditions:

$$L = a R^{b} + c \tag{3.2}$$

## 3.6 SUMMARY

This methodology adopts an empirical, evidence-based approach comprising a literature-based assessment of GEO and LEO satellite technologies, the selection of appropriate latency measurement methods with rainfall data collection onsite, and comparative analysis. The approach also includes latency distribution analysis to distinguish nominal and tail latency regions, followed by the development of rain-induced latency correlation mathematical equations to meet the research objectives.

# CHAPTER FOUR
# RESULT AND DISCUSSION

## 4.1 OVERVIEW

This section focuses on the performance evaluation of the new Low Earth Orbit (Starlink) HTS technology compared to the satellite communication HTS technology of Geostationary Earth Orbit (GEO). Empirical data collected were evaluated with respect to its critical parameters such as latency and rainfall rate impact, resulting in its communication signal link reliability.

The study starts with data preprocessing, which involves cleaning and organizing the collected data, including rainfall intensity and satellite link delay (latency). Next, an analysis is done to find patterns between the rainfall and latency over time, and to create Cumulative Distribution Functions (CDFs) for both rainfall rates and latency for the Starlink LEO and GEO SES-12 satellite systems. Finally, the performance of both satellite links is evaluated by comparing their latency and connection timeouts during different rain conditions. The CDFs are used to calculate useful statistics that help compare how each satellite system handles heavy rain and how reliable they are overall. Given the tropical region's high rainfall intensity and frequency, the empirical observations provide insights into the operational limits and resilience of these technologies under adverse conditions.

These three phases provide a comprehensive performance analysis, highlighting the strengths and limitations of SES-12 GEO HTS and Starlink LEO satellite technologies specifically in tropical environments. Additionally, this analysis establishes a foundation for future research and the development of region-specific recommendations for satellite communication in high-rainfall areas.

## 4.2 EFFECTS OF RAIN ON LATENCY

This section focuses on analysing the performance of the SES-12 GEO HTS and Starlink LEO satellite services during rain events, focusing on how precipitation affects signal latency and discussing the experimental findings in detail.

This section also discusses the correlation between rainfall rate and latency based on experimental data collected under various distinct weather conditions. The study aims to evaluate the impact of rainfall intensity on the Starlink satellite internet system's latency, focusing on signal degradation caused by rain fade.

### 4.2.1 Rain Conditions

The graph consists of two subplots, each analysing the latency performance of SES-12 GEO HTS and Starlink LEO under various rainfall conditions on August 22, 2024. Figure 4.1 and 4.2 highlights the significant impact of heavy rainfall on the latency performance of both SES-12 GEO HTS and Starlink satellite services. High rainfall rate caused the SES-12 GEO HTS VSAT terminal to become fully disconnected at Figure 4.1.

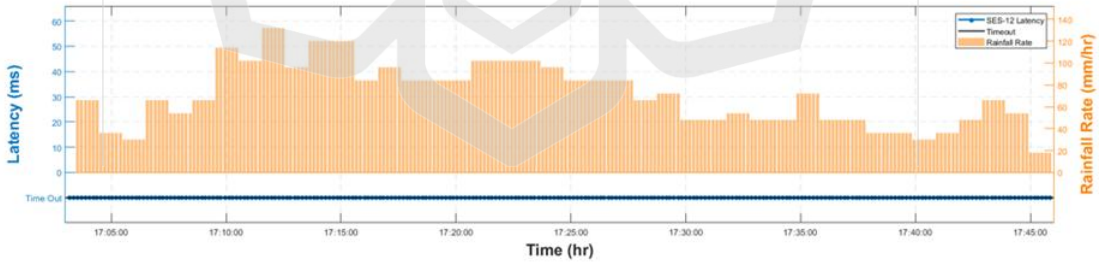



Figure 4.1 A Rain Event occurred on 22 August 2024 for the SES-12 GEO HTS

Rainfall rates consistently exceeded 100 mm/hr, peaking at 120 mm/hr, causing disconnections and latency spikes above 60ms, occasionally exceeding 100ms from the Starlink LEO terminal. This is attributed to the scattering and absorption of satellite signals

by raindrops, highlighting the vulnerability of LEO satellite links to rain fade Figure 4.2.

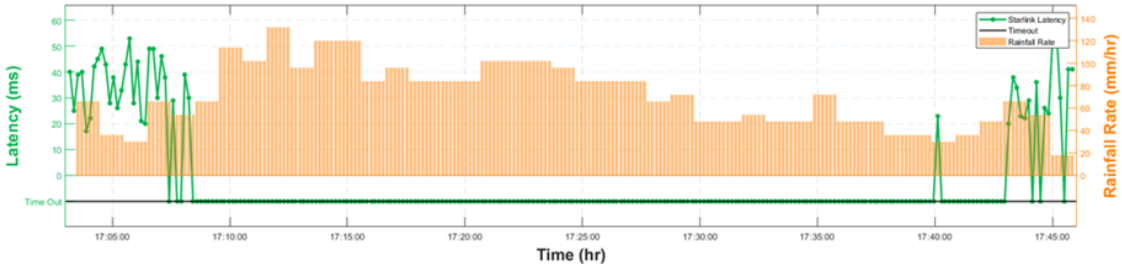



Figure 4.2 A Rain Event occurred on 22 August 2024 for the Starlink LEO

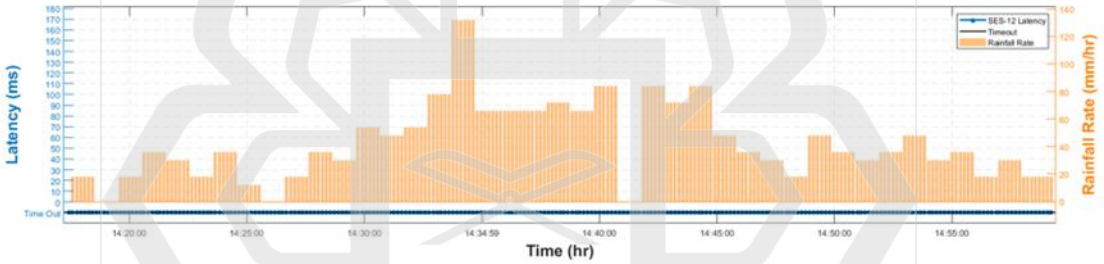



Figure 4.3 A Rain Event occurred on 23 August 2024 for the SES-12 GEO HTS

Figure 4.3 and Figure 4.4 illustrates an event on August 23, 2024, featuring prolonged medium to heavy rainfall with multiple peaks exceeding 100 mm/hr for SES-12 GEO HTS and Starlink LEO VSAT Terminal. During this period in Figure 4.3, the SES-12 GEO HTS VSAT terminal still suffered a total loss of connectivity.

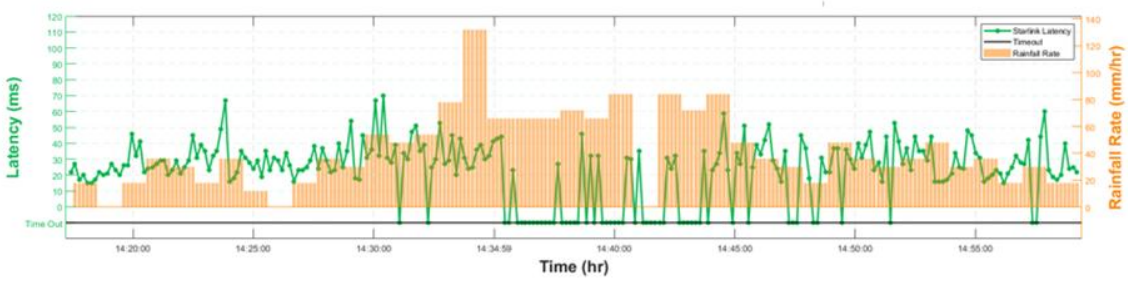



Figure 4.4 A Rain Event occurred on 23 August 2024 for the Starlink LEO

During this period, the Starlink LEO satellite system experienced only a few disconnects as Figure 4.4. In summary, multiple rainfall rate conditions and rain events demonstrate a strong correlation between rainfall intensity with higher latency, highlighting the susceptibility of high-frequency satellite systems to adverse weather. These findings also confirm the vulnerability of Ku-band frequencies to high-intensity rainfall, even in a LEO satellite system mega constellation closer to Earth. Rain fade causes signal degradation and higher latency. However, the Starlink LEO terminal was able to maintain link availability at certain rainfall rates below 60 mm/hr. In contrast, the SES-12 GEO satellite system experienced complete disconnection.

### 4.2.2 Clear sky

The analysis in Figure 4.6 highlights the stable performance of the Starlink satellite system during no rain events, where rainfall rates consistently remained near 0 mm/hr, indicating clear weather conditions. During these periods, latency for Starlink LEO terminal showed minimal variability, remaining within a predictable range between 25ms and 35ms. This stable performance reflects the system's ability to operate optimally in the absence of atmospheric disturbances, with no signal attenuation or interference caused by rain fade.

Compared to GEO satellite services range between 550ms to 750ms in Figure 4.5, Starlink demonstrates greater latency stability in Figure 4.6 under clear skies, showcasing its robustness in favourable weather conditions.

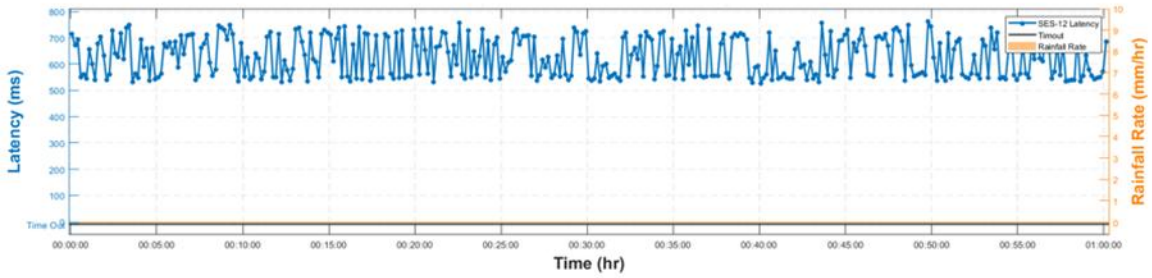



Figure 4.5 A clear sky event occurred on 5 December 2024 for the SES-12 GEO HTS

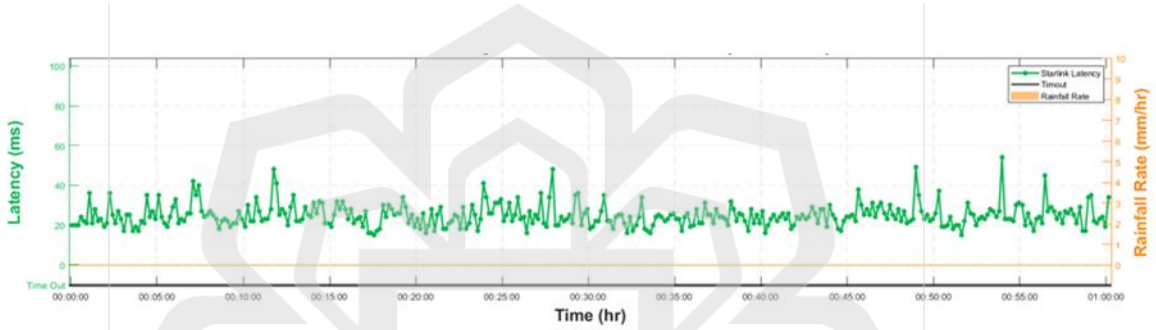



Figure 4.6 A clear sky event occurred on 5 December 2024 for the Starlink LEO

## 4.3 CDF ANALYSIS OF RAIN RATE

The CDF analysis of rainfall, illustrated in Figure 4.7 and 4.8, provides a detailed statistical evaluation of the distribution and frequency of rainfall rates across six months (July to December 2024) and accumulated. This analysis examines the percentage of time that specific rainfall rates are exceeded, offering insights into the occurrence and intensity of precipitation during the data collection period. Each month's rainfall distribution is represented by a distinct line, with the x-axis indicating rainfall rates (in mm/hr) and the y-axis showing the percentage of time exceedance.

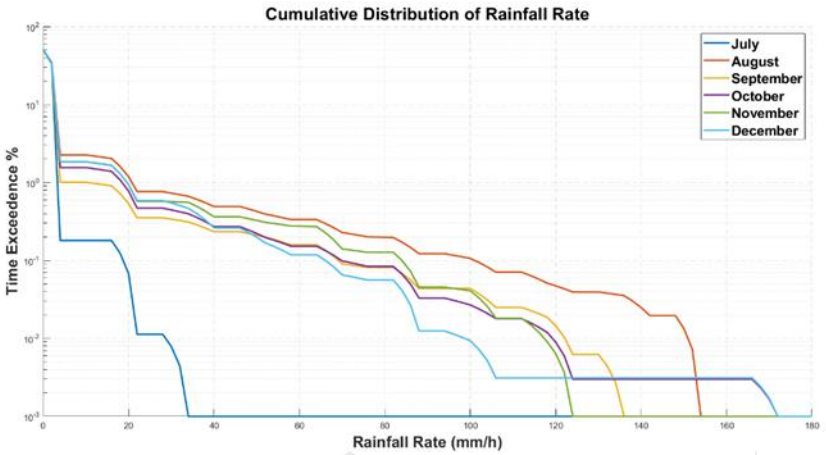



Figure 4.7 CDF Analysis of Rainfall Rate (monthly)

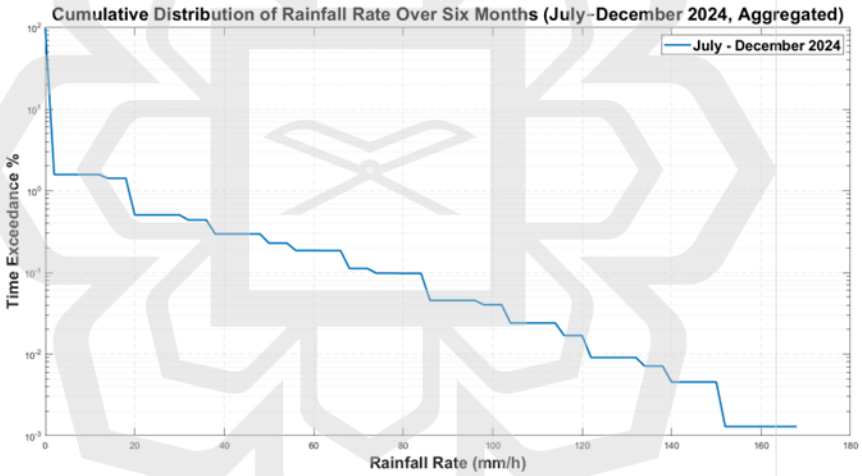



Figure 4.8 CDF Analysis of Rainfall Rate (aggregated)

The cumulative distribution function (CDF) of the rainfall rate in Figure 4.7 highlights seasonal variations in rainfall intensity. The month of July experiences mostly light to moderate rainfall, with minimal heavy rain. From August to November, the probability of moderate-to-heavy rainfall increases, likely due to the monsoon season, as seen in the closely aligned curves. December records the highest extreme rainfall events, exceeding 160 mm/h, but these are rare. Most of the time, rainfall remains in the light-to-

moderate range. Overall, September to November shows the most frequent heavy rain, while December, despite occasional extremes, has a lower time exceedance for intense rainfall. These seasonal variations have a direct impact

On Starlink's performance, particularly in the Ku-band range, as increased rainfall can cause signal attenuation, leading to higher latency, reduced data rates, and potential service disruptions during heavy rain periods. Heavy rainfall events above 100 mm/hr, though infrequent, significantly degrade performance, leading to substantial signal attenuation and increased latency. Moderate rainfall, ranging between 40 and 100 mm/hr, also introduces signal degradation, but connectivity remains mostly intact. In contrast, light rainfall below 40 mm/hr has minimal impact, allowing for stable network performance.

The data collected over a six-month period is not to be directly comparable to ITU-R standards, which are based on long-term averages and focusing on attenuation studies. However, since the data was gathered during the monsoon season, when rainfall is most intense, it still offers valuable insight. Therefore, the result shown estimated $R_{0.01}$ value from Figure 4.8, ranging between 110–130 mm/h, is slightly higher than the value shown by the ITU-R P.837-7 model, which generalizes Malaysia's 0.01% exceedance rainfall rate as 100 mm/h (Ahmad et al., 2024). This suggests that the measured data may reflect localised variations in rainfall intensity that exceed the ITU-R's generalised value.

The study emphasises the importance of using tools like CDF to quantify the likelihood of various rainfall intensities and their correlation with signal degradation. By integrating CDF insights with latency data, a comprehensive understanding of the relationship between rainfall intensity and Starlink system performance is achieved.

## 4.4 CDF ANALYSIS OF LATENCY

The Cumulative Distribution Function (CDF) analysis of latency, as depicted in Figure 4.9 and Figure 4.10, provides a comprehensive evaluation of the percentage of time that

specific latency thresholds were exceeded over six-months period (July to December 2024). This analysis is crucial for assessing the variability and consistency of the Starlink satellite internet system's latency performance under different conditions. By examining the CDF curves, trends in latency distribution across multiple months can be identified, highlighting periods of increased or reduced network delays.

Furthermore, this analysis helps to establish a correlation between latency fluctuations with environmental factors specifically rainfall intensity. The CDF analysis highlights in Figure 4.9 monthly trends in Starlink's latency performance, showing that during July and August, latency averaged at 20ms about 90% of the time. From September to November, latency performance increases closer to 40ms at 90% of the time. These changes in latency performance align with higher rainfall intensities observed in the same period, where rain fade likely caused significant signal attenuation and increased latency.

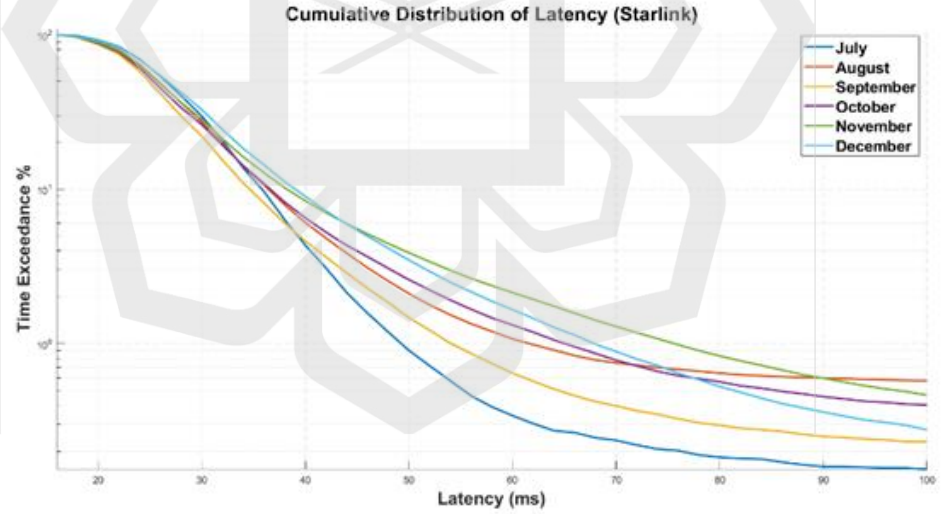



Figure 4.9 CDF Analysis of latency for Starlink LEO (monthly)

December recorded the highest latency, with latency surpassing other months' data. Overall, the aggregated data show in Figure 4.10 that average latency remained below 40ms

for 90% of the time, highlighting the reliability of the Starlink system under varying weather conditions. Understanding these variations is essential for optimising Starlink's quality of service (QoS), predicting network behaviour, and improving system reliability for real-time applications.

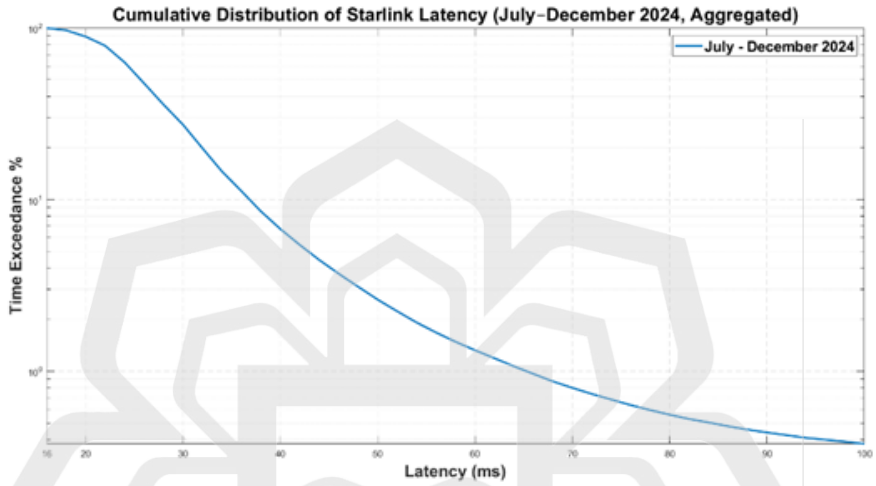



Figure 4.10 CDF Analysis of latency for Starlink LEO (aggregated)

While for SES-12 GEO HTS, as shown in Figure 4.11 and 4.12, the latency averages around 600ms for approximately 90% of the time across the observed six-month period. The cumulative distribution function (CDF) curves in Figure 4.11 indicate that during most months, the latency remains below 1,000ms, suggesting relatively stable performance under normal conditions. However, higher latency values exceeding 1,500ms are occasionally recorded, particularly in October and December, where the curves showed a gradual deterioration beyond this threshold. Notably, in December, the latency remains persistently high, with a significant portion exceeding 2,000 ms, likely due to the extensive rainy season causing network congestion and signal degradation in the GEO satellite link.

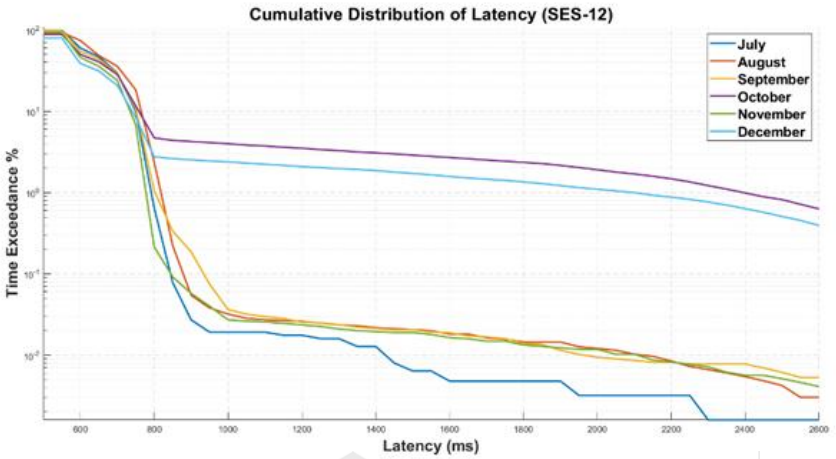



Figure 4.11 CDF Analysis of latency for SES-12 GEO HTS (monthly)

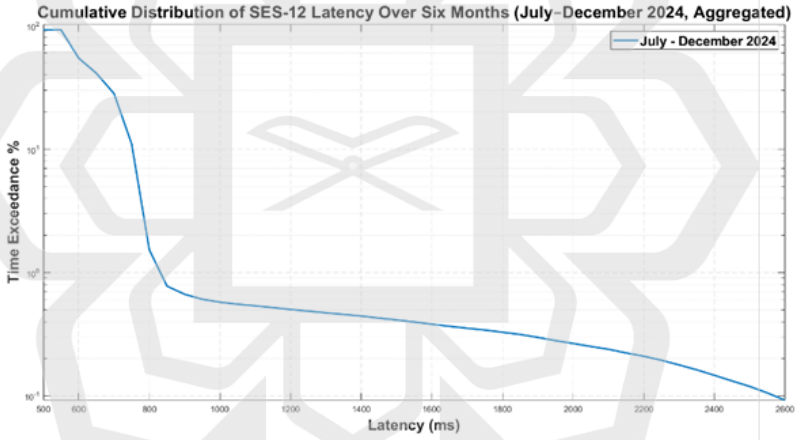



Figure 4.12 CDF Analysis of latency for SES-12 GEO HTS (aggregated)

Overall, the findings established a clear correlation between rainfall intensity and latency performance, emphasising the vulnerability of high-frequency satellite signals to rain fade. The insights gained from this chapter provide a strong foundation for future research aimed at enhancing the resilience and reliability of satellite internet systems in varying environmental conditions.

## 4.5 PERFORMANCE COMPARISON

Figure 4.13 shows a performance comparison graph between the SES-12 GEO HTS and Starlink LEO satellite systems analysing the timeout occurrences and site availability from July to December. The timeout percentage, represented by bars, indicates that Starlink in blue bars consistently experiences minimal timeouts across all months, whereas SES-12 GEO HTS VSAT terminal in red bars shows significantly higher timeout occurrences, particularly in August, November, and December.

On-site availability performance, represented by solid and dashed lines, shows that Starlink in solid blue line maintains above 99% availability throughout the period, highlighting its reliability. In contrast, SES-12 GEO HTS VSAT terminal in the dashed red line exhibits a downward trend in its site availability, with a notable decline in December, where it drops below 90% due to heavy rain events.

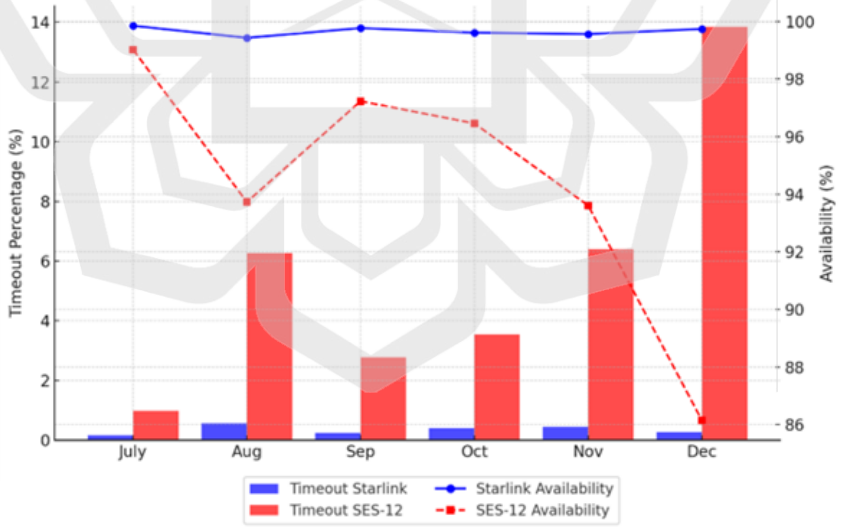



Figure 4.13 Monthly timeout and site availability

Table 4.1 refers to the summary of overall performance analysis indicating that Starlink LEO satellite services maintain superior stability and availability despite using

similar Ku-bands, while SES-12 GEO HTS Satellite services experiences higher disruptions, especially during extreme weather. Starlink LEO terminal shows temporary latency spikes but recovers quickly, whereas the SES-12 GEO HTS VSAT terminal suffers from persistent signal degradation due to rain events. Additionally, Starlink LEO terminal has much lower latency captured at 20ms to 100ms compared to SES-12 GEO HTS VSAT terminal, which is 550ms to 1000ms, further emphasising its advantage in responsiveness. The mean site availability for Starlink LEO terminal remains close to 100%, while SES-12 GEO HTS VSAT terminal fluctuates significantly to 94% for 6 months of the analysis, highlighting its vulnerability to network disruptions in this tropical region.

Table 4.1 Summary of site availability performance evaluation

| **Parameters** | **Starlink LEO terminal** | **SES-12 GEO HTS VSAT terminal** |
|---|---|---|
| Measured Latency | 20-100ms | 550 -3600ms |
| Effect of Rain | Temporary spikes, recovers fast | Persistent degradation |
| Site Availability | 99.63% (6 months average) | 93.99% (6 months average) |

## 4.6 LATENCY TAIL ANALYSIS

Latency is a critical performance metric in satellite communication systems, particularly in applications requiring real-time data transmission. This section presents a comparative latency analysis between Starlink LEO and SES-12 GEO HTS by categorising measured latency into nominal and tail ranges.

At $10^{-2}$ time exceedance level, which in this 6-month dataset corresponds the rainfall rate peaks at approximately 150 mm/hr, driving satellite link latency to around 3.2 seconds. This rare but severe event illustrates the pronounced impact of extreme tropical

downpours on link performance which triggers Adaptive Coding and Modulation (ACM) downgrades, increased packet buffering, and retransmission cycles within the terminal. It's importance of implementing adaptive mitigation strategies for maintaining service quality in high-rainfall regions. GEO systems remain robust under moderate rainfall, with minimal latency deviation across 99% of operational time, consistent with theoretical propagation characteristics.

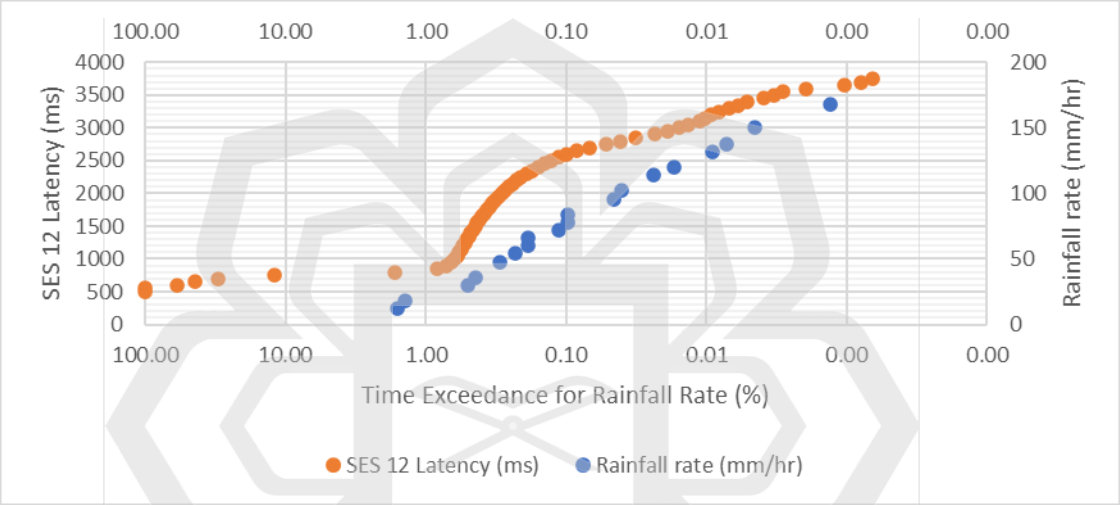



Figure 4.9 Latency tail SES-12 GEO HTS

Conversely, the lower orbital altitude and shorter propagation path of Starlink LEO systems confer a higher degree of resilience, enabling them to maintain near real-time communication capability even under intense rainfall conditions. These findings reinforce the importance of considering orbital configuration in the design and deployment of satellite communication systems intended for high-precipitation tropical environments.

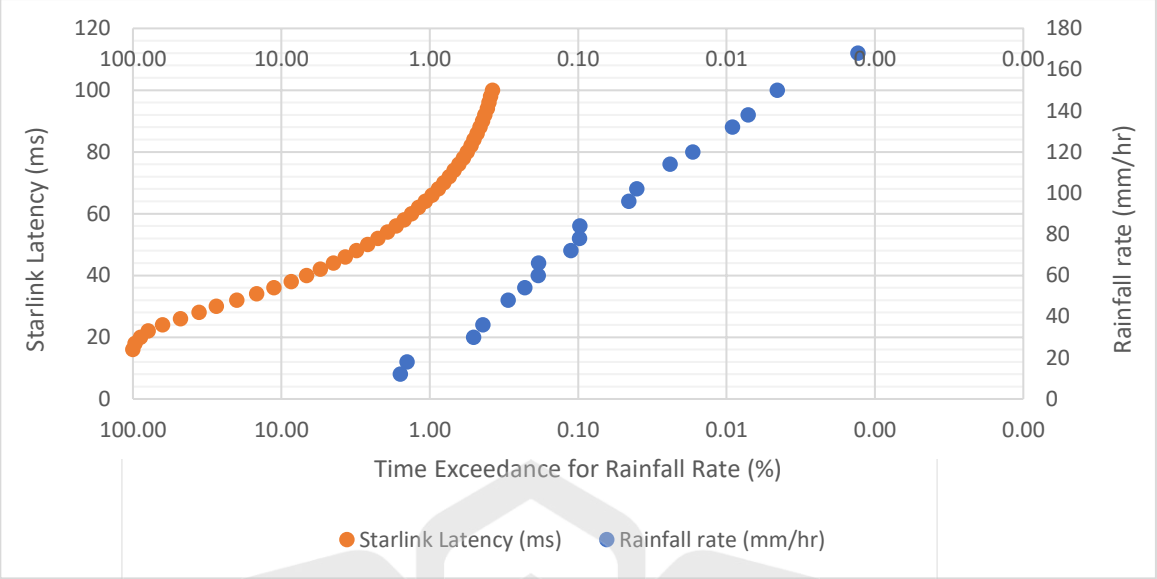



Figure 4.15 Latency tail Starlink LEO

Although rainfall rates of up to approximately 170 mm/hr are observed in Figure 4.15, the corresponding Starlink latency curve remains confined to a lower latency range and does not extend into the extreme tail region observed for the SES-12 GEO HTS link. Consequently, no higher latency points are present at the highest rainfall intensities, as the LEO system maintains low latency without exhibiting a pronounced latency tail under these conditions.

Table 4.2 Latency measurement categories from measured data

| **Parameters** | **SES-12 GEO HTS terminal** | **Starlink LEO terminal** |
|---|---|---|
| Measured Latency | 550 -3600ms | 18-100ms |
| Nominal | 550 -950ms | 18-60ms |
| Tail | > 950ms | >60ms |

The Nominal category represents typical performance under normal conditions, while the Tail category capture outlier latency occurrences which could impact user

experience. Graphical plotting was done to visualize these two distributions separately, allowing a clearer comparison.

The nominal and tail latency boundaries for both satellite systems were defined based on their observed performance distributions and the known physical characteristics of their orbits and network architectures.

### 4.6.1 LEO Starlink Terminal (Low-Earth Orbit)

Starlink consistently demonstrated very low round-trip latency under clear-sky and moderate-rain conditions, with values typically ranging between 18–60 ms for the majority of the measurement period. This range aligns with expected LEO latency performance, where propagation delay is minimal due to the low orbital altitude (~550 km). Latency values above 60 ms represent non-nominal operating conditions where rain attenuation start to affect the link performance.

### 4.6.2 SES-12 GEO HTS VSAT Terminal (Geostationary Orbit)

For the GEO link, latency behavior is fundamentally different due to the much higher propagation delay associated with geostationary orbit which at 36,00km altitude. Under clear-sky and moderate-rain conditions, SES-12 latency remained within 550–950 ms, forming the nominal operating region. Latency values exceeding 950 ms correspond to periods of rain-fade-induced particularly during intense tropical rainfall. Unlike the LEO system, the GEO terminal does not always fully disconnect during extreme rain events. Instead, it becomes intermittent alternating between periods of very high latency and timeout responses. Although the link technically remains active at times, the connection is highly unstable and not usable for real-time applications under these deep-fade conditions.

## 4.7 EQUATION AND CORRELATION

The latency data was correlated in two categories, Nominal Latency and Tail Latency. This separation was necessary because the latency behaviour under normal operating conditions (nominal) is fundamentally different from the extreme degradation during heavy rain (tail). Using a single correlation would bias the regression toward nominal conditions and fail to accurately represent worst-case service behaviour.

The correlation was performed using the MATLAB Curve Fitter Toolbox (Curve Fitting App), where several curve types were evaluated, including logarithmic, power, and exponential methods. MATLAB automatically calculated goodness of fit statistics such as the coefficient of determination ($R^2$), Root Mean Square Error (*RMSE*), and Sum of Squared Errors (*SSE*) to determine the most suitable fit.

Nominal latency was best represented using a power-law or logarithmic fit, due to its smooth and gradual trend. In contrast, Tail latency shows a strong non-linear, steep escalation, which was most accurately correlated using a power square function of the form:

$$f(x) = ax^b + c \tag{4.1}$$

where $x$ represent the time exceedance probability, and latency increases rapidly as $x$ approaches rare events. Only the best performing methods, identified by highest $R^2$ and the lowest *RMSE* were selected for final use in the rainfall latency correlation analysis.

### 4.7.1 Rainfall Rate Logarithmic Curve Fit

The rainfall rate was correlated as a logarithmic function of the time exceedance percentage. The fitted curve shows that rainfall intensity decreases sharply at very low exceedance probabilities and gradually flattens as the exceedance increases. This behaviour reflects the typical tropical rainfall distribution, where extremely high rainfall rates occur

only during rare, short duration events. MATLAB's Curve Fitting App was used to analyse the measured rainfall data and generate the fitted equation. The data points (rainfall vs. exceedance percentage) were imported into the App, and several curve types were evaluated to identify the most suitable correlation. Among the tested functions, the logarithmic curve fit demonstrated the best agreement with the measured data and was therefore selected. MATLAB automatically calculated the parameters, best-fit curve, and fit quality metrics (such as $R^2$), and the App enabled visual inspection to ensure the fitted curve accurately represented the empirical trend. Once the optimal logarithmic correlation was confirmed, MATLAB generated the final mathematical equation used in this thesis to characterise the rainfall exceedance behaviour.

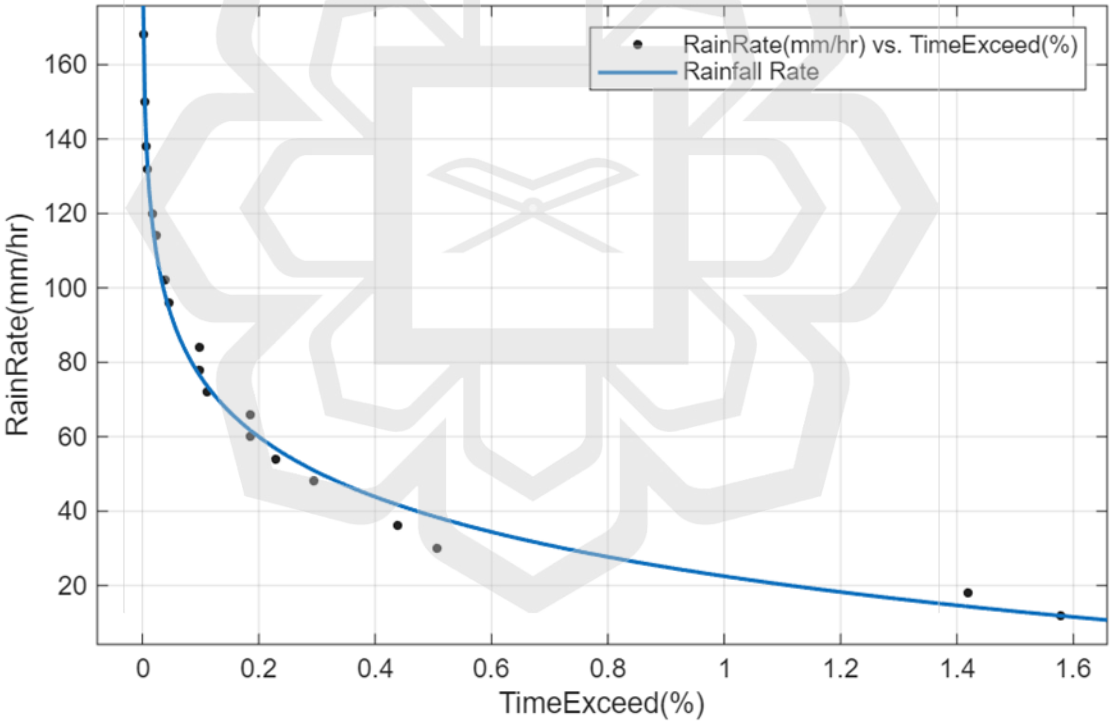



Figure 4.16 Rainfall Rate Logarithmic Curve Fit

The empirical relationship between the **rainfall rate** and the **time exceedance probability** was derived using a logarithmic regression correlation of the form.

$$f(x) = a\ log(x) + b \quad (4.2)$$

Where $f(x)$ represents the rainfall rate (mm/h), $x$ is the percentage of time exceedance (%), and $a$ and $b$ are regression coefficients determined through curve fitting.

Based on the measured rainfall data and regression analysis, the derived logarithmic equation is expressed as shown in Equation (4.3).

$$R_{Rainfall\ rate} = -23.28\ log(x) + 22.52 \quad (4.3)$$

where $R_{Rainfall\ rate}$ represents the rainfall rate (mm/h) and $x$ represents the percentage of time during which that rainfall rate is exceeded.

The negative coefficient $(-23.28)$ indicates that the rainfall rate decreases logarithmically as the exceedance probability increases. This means that high rainfall intensities occur only for short durations, while lower rainfall intensities occur more frequently.

### 4.7.2 Rainfall Rate correlation with SES-12 GEO HTS Nominal

Figure 4.17 illustrates the correlation between the measured rainfall rate and the SES-12 nominal round-trip time (RTT) under clear-sky and rain-affected conditions. The empirical data points (black dots) represent the observed RTT values plotted against the time exceedance percentage, while the blue curve shows the fitted regression correlation that characterizes the nominal latency behaviour of the GEO satellite link.

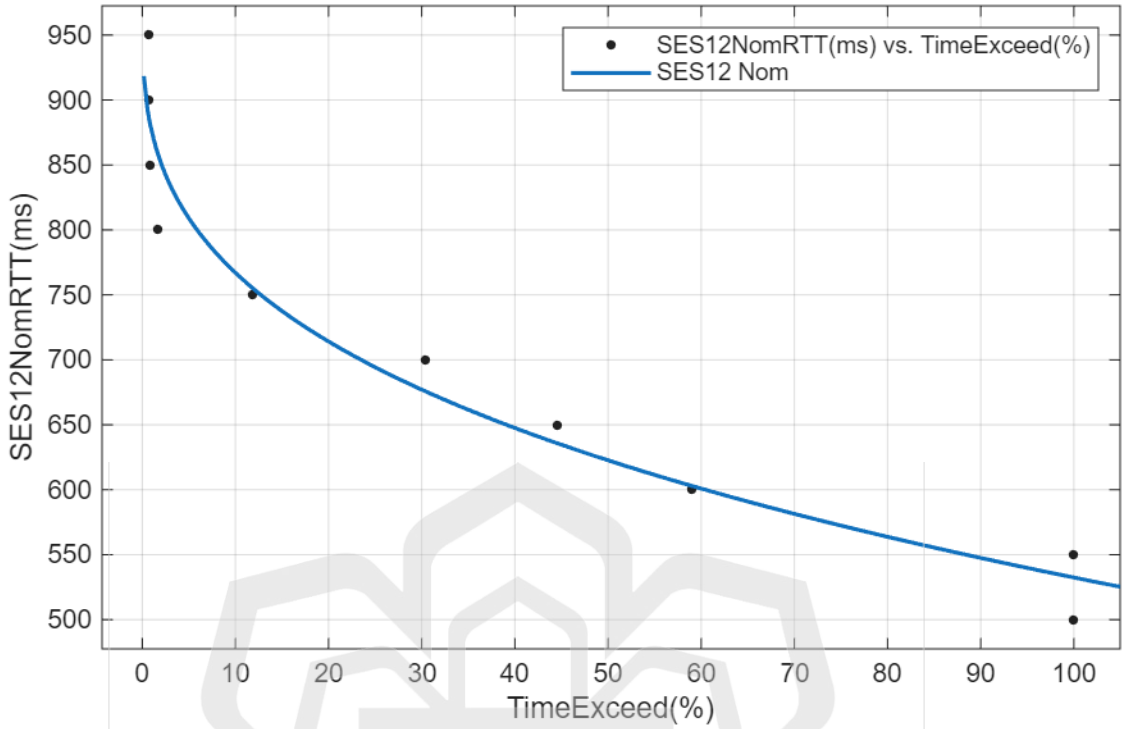



Figure 4.17 SES-12 GEO HTS Tail Power Curve Nominal

SES-12 Nominal Power Curve Fit (power square) The empirical relationship between the **rainfall rate** and the **time exceedance probability** was derived using a logarithmic regression correlation of the form.

$$f(x) = a\,x^{(b)} + c \tag{4.4}$$

Where $f(x)$ represents the rainfall rate (mm/h), $x$ is the percentage of time exceedance (%), $a$ and $(b)$ are regression coefficients determined from curve fitting.

$$f(x) = -95.24\,x^{(0.33)} + 971.49 \tag{4.5}$$

The **rainfall rate (R)** and SES-12 nominal **latency (L)** are correlate as functions of the exceedance probability $x$:

$$R = -23.28 \log(x) + 22.52 \tag{4.6}$$

Where $L_{Nom\,Geo}$ is the nominal latency in milliseconds (ms) and $x$ is the time-exceedance percentage (%). The negative coefficient indicates that latency decreases slightly as exceedance percentage increases, showing that **higher delays occur less frequently**, mainly during clear-sky or low-rain conditions.

$$L_{Nom\,Geo} = -95.24\,x^{0.33} + 971.49 \tag{4.7}$$

To express **latency (L)** directly in terms of **rainfall rate (R)**, first eliminate $x$ from the equations. Starting from the rainfall equation:

$$\log(x) = \frac{22.52 - R}{23.28} \tag{4.8}$$

$$x = 10^{\frac{22.52-R}{23.28}} \tag{4.9}$$

Substituting this expression into the SES-12 nominal latency equation:

$$L_{Nom\,Geo} = -95.24 \times (10^{\frac{22.52-R}{23.28}})^{0.33} + 971.49 \tag{4.10}$$

Simplify the exponent term:

$$L_{Nom\,Geo} = -95.24 \times 10^{0.33(\frac{22.52-R}{23.28})} + 971.49 \tag{4.11}$$

Final correlation equation:

$$L_{Nom\,Geo} = -95.24 \times 10^{(\frac{-0.33}{23.28}(R-22.52))} + 971.49 \tag{4.12}$$

### 4.7.3 Rainfall Rate correlation with SES-12 GEO HTS Tail

Correlation between measured rainfall rate and SES-12 GEO tail RTT under severe rain-fade conditions. The black dots represent the observed RTT data points plotted against

the time-exceedance percentage, while the blue curve shows the Power Curve Fit regression correlation used to characterise the tail latency behaviour of the SES-12 link. The fitted curve illustrates the sharp, non-linear increase in latency that occurs as exceedance probability decreases, indicating the onset of heavy rainfall and deep-fade conditions. This pattern reflects the effect of rain-induced attenuation, adaptive coding and modulation (ACM) downgrades, and buffering delays that dominate the GEO system's performance during extreme tropical rain events.

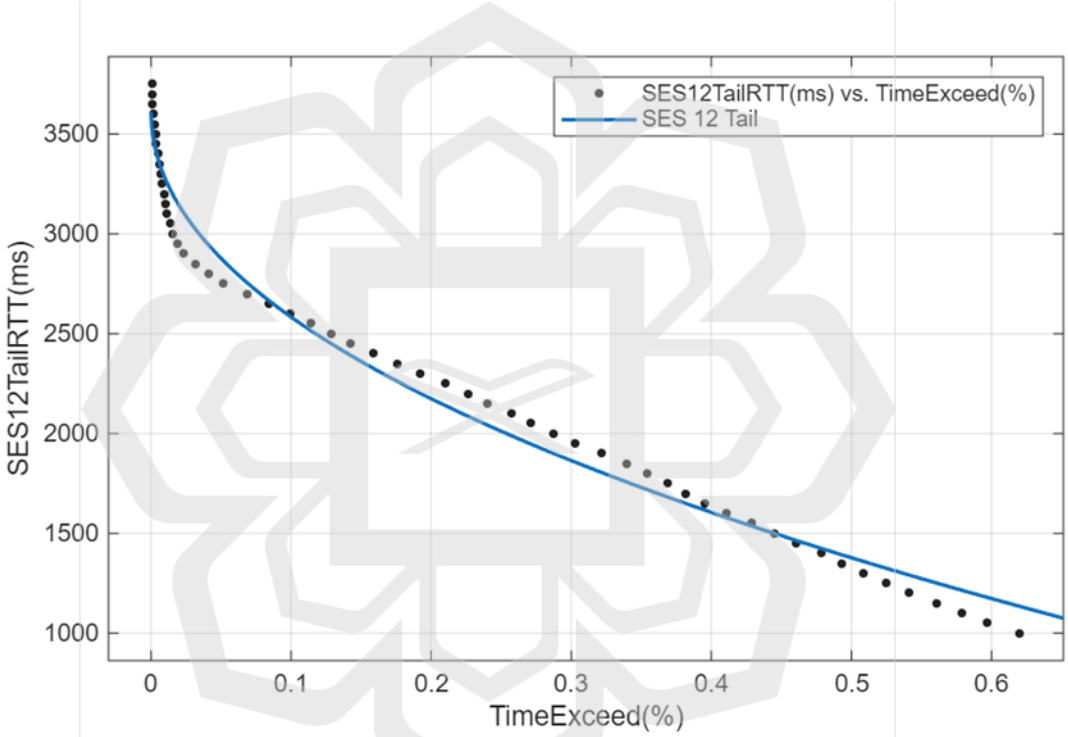



Figure 4.10 SES-12 GEO HTS Tail Power Curve Fit

The empirical relationship between the **rainfall rate** and the **time exceedance probability** for SES-12 Tail Power Curve Fit was derived using a logarithmic regression correlation of the form, referring to equation (4.4).

Where $f(x)$ represents the rainfall rate (mm/h), $x$ is the percentage of time exceedance (%), $a$ and $(b)$ are regression coefficients determined from curve fitting.

$$f(x) = -3129.9\, x^{(0.48)} + 3625.2 \quad (4.13)$$

To express **latency (L)** directly as a function of **rainfall rate (R)**, the variable $x$ is eliminated similarly as per equation (4.8) and (4.9). Substitute this into the SES-12 tail latency, $L_{Tail\ Geo}$ equation:

$$L_{Tail\ Geo} = -3129.9 \times (10^{\frac{22.52-R}{23.28}})^{0.48} + 3625.2 \quad (4.14)$$

Simplify the exponential term:

$$L_{Tail\ Geo} = -3129.9 \times 10^{0.48(\frac{22.52-R}{23.28})} + 3625.2 \quad (4.15)$$

Final correlation equation:

$$L_{Tail\ Geo} = -3129.9 \times 10^{(\frac{-0.48}{23.28}(R-22.52))} + 3625.2 \quad (4.16)$$

### 4.7.4 Rainfall Rate correlation with Starlink LEO Latency Nominal

Figure 4.19 illustrates the relationship between the rainfall-rate exceedance and the nominal latency performance of the Starlink LEO satellite system. The data were fitted using a **power-law regression formula**, commonly applied for non-linear relationships between exceedance probability and latency behaviour in low-Earth-orbit constellations.

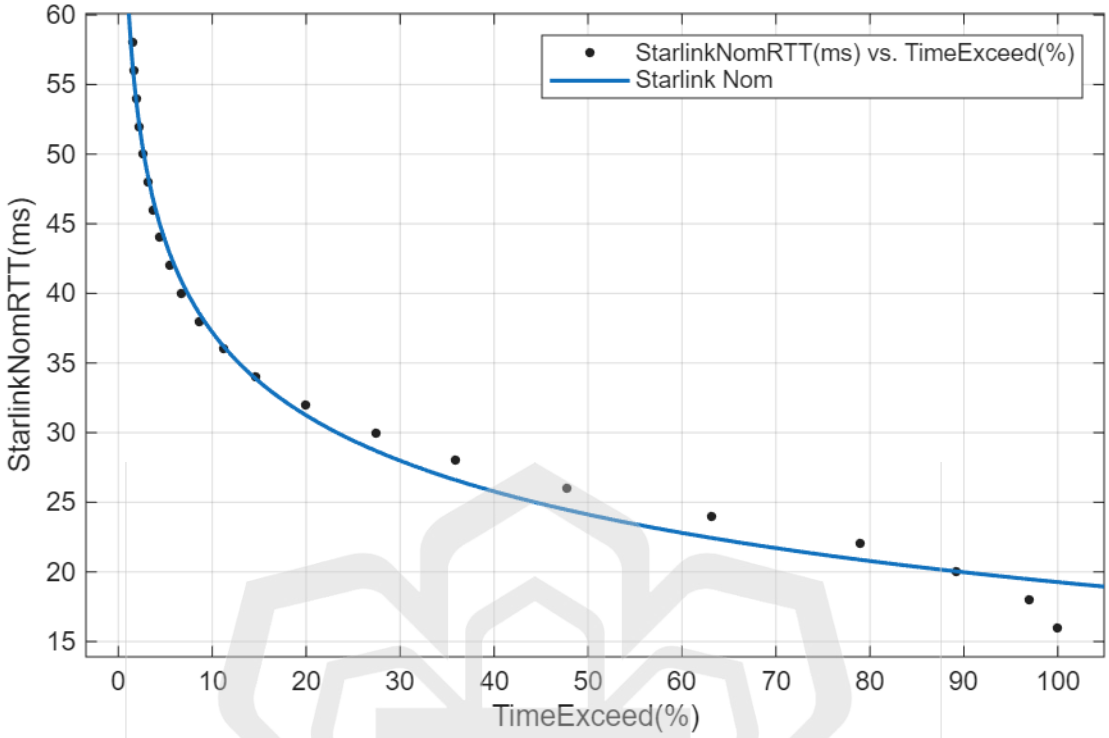



Figure 4.19 Starlink LEO Nominal Power Curve Fit

The empirical relationship between the **rainfall rate** and the **time exceedance probability** for Starlink LEO Nominal Power Curve Fit was derived using a logarithmic regression correlation of the form, referring to equation (4.4).

Where $f(x)$ represents the rainfall rate (mm/h), $x$ is the percentage of time exceedance (%), $a$ and $(b)$ are regression coefficients determined from curve fitting.

$$f(x) = 94.05\, x^{(-0.129)} + 32.68 \tag{4.17}$$

To express **latency (L)** directly as a function of **rainfall rate (R)**, the variable $x$ is eliminated as per equation (4.8) and (4.9). Substitute this expression for $x$ into the latency equation:

$$L_{Nom\,Leo} = 94.05(10^{\frac{22.52-R}{23.28}})^{-0.129} - 32.68 \tag{4.18}$$

Simplify the exponent term:

$$L_{Nom\ Leo} = 94.05 \times 10^{-0.129(\frac{22.52-R}{23.28})} - 32.68 \quad (4.19)$$

Final correlation equation:

$$L_{Nom\ Leo} = 94.05 \times 10^{(\frac{0.129}{23.28}(R-22.52))} - 32.68 \quad (4.20)$$

### 4.7.5 Rainfall Rate correlation with Starlink LEO Latency Tail

Figure 4.20 illustrates the relationship between the rainfall-rate exceedance and the tail latency performance of the Starlink LEO satellite system. The data were fitted using a **power-law regression formula**, commonly applied for non-linear relationships between exceedance probability and latency behaviour in low-Earth-orbit constellations.

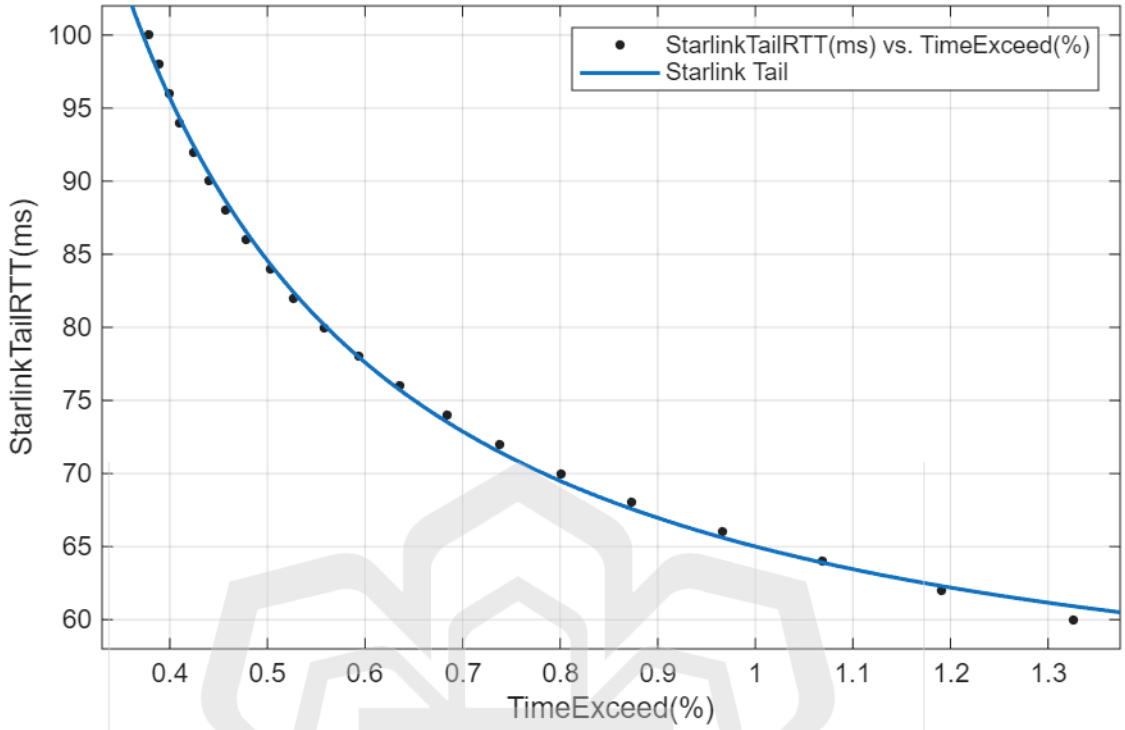



Figure 4.11 Starlink LEO Tail Power Curve Fit

The empirical relationship between the **rainfall rate** and the **time exceedance probability** for Starlink LEO Power Curve Fit was derived using a logarithmic regression formula of the form, referring to equation (4.4).

Where $f(x)$ represents the rainfall rate (mm/h), $x$ is the percentage of time exceedance (%), $a$ and $(b)$ are regression coefficients determined from curve fitting.

$$f(x) = 13.22\, x^{(-1.31)} + 51.78 \tag{4.21}$$

To express **latency (L)** directly as a function of **rainfall rate (R)**, the variable $x$ is eliminated as per equation (4.8) and (4.9). Substitute this into the LEO Starlink tail latency equation:

$$L_{Tail\ Leo} = 13.22(10^{\frac{22.52-R}{23.28}})^{-1.31} + 51.78 \tag{4.22}$$

Simplify the exponential term:

$$L_{Tail\ Leo} = 13.22 \times 10^{-1.31(\frac{22.52-R}{23.28})} + 51.78 \quad (4.23)$$

Final correlation equation:

$$L_{Tail\ Leo} = 13.22 \times 10^{(\frac{1.31}{23.28}(R-22.52))} + 51.78 \quad (4.24)$$

## 4.8 SUMMARY OF MAJOR FINDING

This section summarizes the principal outcomes obtained from the six-month measurement and subsequent data analysis. The research focused on understanding how tropical rainfall influences the latency performance of High-Throughput Satellite (HTS) in the Ku-band, comparing SES-12 GEO HTS system and a LEO Starlink system. The findings presented here highlight the key performance differences between both systems under clear-sky and rain-fade conditions, the observed latency ranges and link availability, as well as the development of empirical rain-induced latency correlation. These results collectively address the study's objectives and provide a quantitative foundation for analysing satellite link behaviour in tropical climates.

### 4.8.1 GEO Latency Characteristics (SES-12)

- SES12 GEO HTS terminal exhibited nominal latency values between 550 ms and 950 ms, consistent with the expected propagation delay of a geostationary satellite system.
- Under heavy tropical rainfall, latency increased sharply reaching up to 3,600 ms, signifying the onset of tail-latency conditions.
- Link availability decreased to 94%, mainly due to prolonged rain fade and adaptive coding and modulation (ACM) downgrades in the tropical rainfall.

### 4.8.2 LEO Starlink Latency Characteristics

- LEO Starlink terminal maintained significantly lower latency values, ranging from 18 ms to 100 ms, with nominal operation between 18–60 ms.
- Only brief tail-latency events were observed above 60 ms, typically during short bursts of intense rain or satellite handovers.
- Overall link availability reached **99.6%**, demonstrating strong resilience to rain fade and rapid recovery after short disruptions.

### 4.8.3 Rain Induced Latency Correlation

Empirical relationships were derived using **power** and **logarithmic** curve fitting techniques to directly relate rainfall rate ($R$) to latency ($L$) for both nominal and tail. Rain-induced latency correlation is given as follows:

Table 4.3 Rain-induced latency correlation

| Rain-induced Correlation | Equations |
|---|---|
| SES-12 Nominal | $L_{Nom\ Geo} = -95.24 \times 10^{(\frac{-0.33}{23.28}(R-22.52))} + 971.49$ |
| SES-12 Tail | $L_{Tail\ Geo} = -3129.9 \times 10^{(\frac{-0.48}{23.28}(R-22.52))} + 3625.2$ |
| Starlink Nominal | $L_{Nom\ Leo} = 94.05 \times 10^{(\frac{0.129}{23.28}(R-22.52))} - 32.68$ |
| Starlink Tail | $L_{Tail\ Leo} = 13.22 \times 10^{(\frac{1.31}{23.28}(R-22.52))} + 51.78$ |

These equations capture the nominal and tail latency behaviours for both GEO and LEO systems under various rainfall intensities.

The findings confirm that GEO systems experience substantial latency expansion under heavy rainfall. This occurs due to rain-induced signal attenuation, which triggers ACM downgrades, retransmissions, and queueing delays, thereby prolonging RTT. In contrast, LEO systems show minimal latency variation due to their low orbital altitude and dynamic multi-satellite routing capability.

The derived rain-induced latency correlation provides a quantitative representation of these behaviours, allowing prediction of latency response based only on rainfall rate. This provides a quantitative foundation for developing weather adaptive satellite communication link strategies within GEO and LEO, especially in tropical regions where rainfall occurs frequently and with high intensity.

# CHAPTER FIVE

# CONCLUSION

## 5.1 CONCLUSION

This work has demonstrated in detail that tropical rainfall demonstrates a significant measurable influence on satellite communication latency, with the effect being far more noticeable for Geostationary High Throughput Satellites (GEO HTS) than for Low Earth Orbit (LEO) systems. Through extensive empirical data collection, statistical analysis, and curve-fitting using logarithmic and power-law approaches, the study confirms that rain-induced latency degradation is a real operational challenge in tropical regions, where rainfall intensities commonly exceed 50–100 mm/h where rain events occur frequently throughout the year.

The proposed empirical correlation successfully establishes a clear relationship between rainfall rate and latency behaviour. For tropical GEO links such as SES-12, the latency exhibited a strong upward trend under rain conditions, rising sharply during high rainfall periods. The rainfall rate correlation, derived from a logarithmic regression, accurately represented the distribution of rainfall intensities over time, while the SES-12 latency correlation (nominal and tail) revealed distinct characteristics of GEO link behaviour. While the tail latency correlation, in particular, showed a steep increase at very low exceedance levels, reflecting the rare but severe delays associated with heavy rain, signal fading, link adaptation processes, and increased re-transmissions.

The results show that GEO latency can exceed 1000–3600 ms during periods of intense rainfall, indicating the combined effects of propagation delay, queueing, congestion, and rain-fade mitigation mechanisms implemented by the gateway and modem. The exponential-like increase in SES-12 latency under heavy rain further emphasises the sensitivity of GEO links to atmospheric attenuation, especially for Ka-band and HTS spot beams commonly deployed over Malaysia and the surrounding tropical belt. These findings

confirm that rain attenuation does not only reduce signal strength but also impacts user-perceived latency, round-trip time (RTT), and overall quality of service.

In contrast, the analysis of Starlink LEO performance indicated a markedly different behaviour. The LEO latency remained consistently low and stable across all rainfall intensities, typically ranging between 18 and 60 ms under both clear-sky and moderate rain conditions. Even during strong rainfall events, the latency increase was minimal and short-lived, with rapid recovery immediately after the rain subsided. This behaviour highlights Starlink's inherent advantages of short propagation path length, rapid satellite handover, multi-satellite routing, and adaptive path selection. Because LEO systems operate at much lower altitudes (500–550 km compared to GEO's 36,000 km), they avoid the long propagation delay that dominates GEO latency, enabling more resilient performance even when rain temporarily affects individual beams or satellites.

The comparative analysis therefore shows a clear contrast between GEO and LEO systems under tropical rainfall conditions. GEO systems experience substantial latency variation due to their reliance on a single satellite and longer delay budget, while LEO systems inherently mitigate latency issues through their architectural design. The correlation developed in this study highlight this contrast by quantifying the latency behaviour for each system across different rainfall rates and exceedance probabilities.

These results lead to an important conclusion where GEO and LEO architectures exhibit complementary strengths. GEO HTS provides wide-area coverage, high capacity, and stable throughput for broadcast and enterprise use cases, but it remains sensitive to rain-induced latency spikes. LEO systems, on the other hand, deliver low-latency, high-availability connectivity and recover quickly from rain events, but may have coverage limitations in certain regions. By combining both systems in a hybrid or multi-orbit architecture, network operators can achieve a more resilient and adaptive satellite communication solution, particularly in high-rainfall tropical climates.

The study therefore supports the potential of multi-orbit satellite networks where

GEO is leveraged for capacity and coverage, while LEO serves latency-critical or weather-affected traffic. Such hybrid designs offer improved performance, especially for applications such as cloud access, video conferencing, remote operations, and mobile backhaul in regions prone to heavy rain. Ultimately, the findings demonstrate that understanding the quantitative relationship between rainfall and latency is essential for satellite operators, network engineers, and service providers planning robust, next-generation connectivity solutions for tropical environments.

## 5.2 PRACTICAL IMPLICATION

The rain-induced latency correlation developed in this study provide practical value for improving satellite network planning and operation in tropical regions. For GEO networks such as SES-12, the correlation helps engineers estimate fade margins, plan Quality of Service (QoS) levels, and design link budgets that consider potential latency increases during heavy rainfall. These correlations also support better configuration of adaptive coding and modulation (ACM), allowing GEO systems to anticipate performance degradation and maintain service continuity as rain intensity changes.

For LEO Satellite systems such as Starlink, the results can assist in optimising satellite handover timing, network scheduling, and routing decisions under short-term weather variations. The findings also support the development of hybrid GEO–LEO architectures, where traffic can be dynamically switched between orbits to maintain low latency and minimise service disruptions during adverse weather. Overall, the finding correlations offer a useful foundation for weather-aware satellite link management and performance optimisation in high-rainfall tropical environments.

## 5.3 FUTURE WOKS

To expand upon this research, several recommendations are proposed. First, future studies should extend data collection across multiple geographic locations and different climate zones to validate and refine the rain-induced latency correlations, ensuring their broader applicability beyond a single tropical site. Additionally, it is recommended to conduct multi-frequency investigations, particularly in the Ka-, Q-, and V-bands, to compare how rain fade affects different satellite operating bands and to identify frequency-dependent latency behaviours.

Further work should also explore GEO–LEO hybrid integration strategies, where intelligent traffic routing decisions are made based on real-time latency measurements or weather conditions, potentially improving overall network resilience during adverse weather. Future studies may also investigate how such adaptive routing mechanisms can be aligned with emerging 6G Non-Terrestrial Network (NTN) architectures, in which satellite systems are expected to operate as an integral component of the terrestrial–non-terrestrial communication framework. In this context, rain-aware latency models could support dynamic network slicing, quality-of-service differentiation, and cross-layer optimization in 6G NTN enabled satellite networks.

Finally, researchers are encouraged to examine the impact of rain fade on throughput and packet loss, alongside latency, to develop a more comprehensive Quality of Service (QoS) assessment correlation for satellite communication systems. Extending this analysis within a 6G NTN perspective would enable more accurate performance prediction and intelligent resource management for next-generation satellite–terrestrial integrated communication systems

# REFERENCES


Y. Guan, F. Geng, and J. H. Saleh, "Review of high throughput satellites: Market disruptions, affordability-Throughput map, and the cost per bit/second decision tree," 2019.

Euroconsult, "High Throughput Satellites are entering a new era of accelerated and drastic transformation," *Directions Magazine*, Mar. 2022.

P. Inigo *et al.*, "Review of Terabit/s satellite, the next generation of HTS systems," in *2014 7th Advanced Satellite Multimedia Systems Conference and the 13th Signal Processing for Space Communications Workshop, ASMS/SPSC 2014*, 2014.

M. Centenaro, C. E. Costa, F. Granelli, C. Sacchi, and L. Vangelista, "A survey on technologies, standards and open challenges in satellite IoT," 2021.

Ogutu B. Osoro and Edward J. Oughton, "A Techno-Economic Framework for Satellite Networks Applied to Low Earth Orbit Constellations: Assessing Starlink, OneWeb and Kuiper," *IEEE Access*, vol. 9, Oct. 2021.

J. Dvořák, J. Hart, and J. Kumhálová, "Atmospheric attenuation of the ku band along the space-earth path due to clouds and rain," *Agronomy Research*, vol. 18, no. Special Issue 2, 2020.

O. Kodheli *et al.*, "Satellite Communications in the New Space Era: A Survey and Future Challenges," 2021.

Y. Maekawa *et al.*, "Effects of tropical rainfall to the Ku-band satellite communications links at the Equatorial Atmosphere Radar Observatory," *Journal of the Meteorological Society of Japan*, vol. 84, no. SPEC. ISS., 2006.

M. Edirisinghe, N. Alahacoon, M. Ranagalage, and Y. Murayama, “Long-Term Rainfall Variability and Trends for Climate Risk Management in the Summer Monsoon Region of Southeast Asia,” *Advances in Meteorology*, vol. 2023, pp. 1–12, Oct. 2023.

TECH COLLECTIVE, “Is Malaysia poised to become a player in the spacetech?,” Mar. 2023.

Q. Pan, G. H. Bryant, J. McMahon, J. E. Allnutt, and F. Haidara, “High elevation angle satellite-to-earth 12 GHz propagation measurements in the tropics,” *International Journal of Satellite Communications*, vol. 19, no. 4, 2001.

J. S. Mandeep and S. I. S. Hassan, “Slant-path rain attenuation predictions in tropical regions,” *J Atmos Sol Terr Phys*, vol. 68, no. 8, 2006.

UN Office for the Coordination of Humanitarian Affairs (OCHA), “Asia Pacific Regional Reference Map: Annual Precipitation.” Accessed: Mar. 09, 2025. [Online]. Available: https://reliefweb.int/map/world/asia-pacific-regional-reference-map-annual-precipitation

J. Deutschmann, K. S. Hielscher, and R. German, “Broadband Internet Access via Satellite: Performance Measurements with different Operators and Applications,” in *Breitbandversorgung in Deutschland - 16. ITG-Fachkonferenz*, 2022.

O. Vidal, B. Roy, S. Dimitrov, R. Barrios, D. Giggenbach, and A. Le Kernec, “Next generation high throughput satellite system based on optical feeder links,” *https://elib.dlr.de/*, 2015.

F. Geng, D. B. Gomez, Y. Guan, and J. H. Saleh, “Monte-Carlo value analysis of high-throughput satellites: Value levers, tradeoffs, and implications for operators and investors,” *PLoS One*, vol. 14, no. 9, 2019.

Christopher McLain and Janet King, “Future Ku-Band mobility satellites,” in *35th AIAA International Communications Satellite Systems Conference, ICSSC 2017*.

S. E. Hobbs, J. P. Sanchez, and J. Kingston, “Extended lifetime Laplace plane Geo SAR mission design,” in *IET Conference Publications*, 2015.

NBN Co, “Administration of the National Broadband Network Satellite Support Scheme,” Nov. 2017.

Shagun Sachdeva. (2018). HTS MEO-/LEO Constellations’ Impact on GEO Satellite. https://apscc.or.kr/wp-content/uploads/2018-APSCC-Q4-web.pdf

SES, “SES-12 satellite to serve Asia-Pacific and Middle East,” https://developingtelecoms.com/.

SES S.A., “SES-12 at 95 degree East,” https://www.ses.com/our-coverage#/explore/satellite/365.

Sonata, I., Sandra Octaviani, B. W., & Iskandar, I. (2020). Mitigating the effect of rain fading on ka band high throughput satellite in indonesia: An empirical study. *International Journal of Scientific and Technology Research*, *9*(3).

Jason Rainbow, “Amazon gets key FCC approval for more than 3,000 LEO broadband satellites,” *Spacenews*, Feb. 08, 2023.

S. Agnelli, P. Feltz, P. F. Griffiths, and D. Roth, “Satellite’s role in the penetration of broadband connectivity within the European Union,” in *2014 7th Advanced Satellite Multimedia Systems Conference and the 13th Signal Processing for Space Communications Workshop, ASMS/SPSC 2014*, 2014.

S. Ma, Y. C. Chou, H. Zhao, L. Chen, X. Ma, and J. Liu, “Network Characteristics of LEO Satellite Constellations: A Starlink-Based Measurement from End Users,” in *Proceedings - IEEE INFOCOM*, 2023.

S. W. Powell, R. A. Houze, and S. R. Brodzik, “Rainfall-type categorization of radar echoes using polar coordinate reflectivity data,” *J Atmos Ocean Technol*, vol. 33, no. 3, 2016.

C. Han *et al.*, “Characteristics of rain-induced attenuation over signal links at frequency ranges of 25 and 38 ghz observed in beijing,” *Remote Sens (Basel)*, vol. 13, no. 11, 2021.

Y. A. Ahmad, A. F. Ismail, M. N. A. Abdul Hamid, and M. F. Jamlos, “Area-Based Rainfall Rate Model for Specific Attenuation in the Equatorial Region,” *IIUM Engineering Journal*, vol. 25, no. 2, pp. 287–298, Jul. 2024.

J. D. Nor Hisham Haji Khamis, “Rainfall Rate from Meteorological Radar Data for Microwave Applications in Malaysia,” in *2005 13th IEEE International Conference on Networks Jointly held with the 2005 IEEE 7th Malaysia International Conf on Communic*, IEEE, 2005, pp. 1008–1010.

Ajayi Taiwo Seun, “Mobile Satellite Communications,” Blekinge Institute of Technology, 2007.

“ITU-R P618.14,” *Propagation data and prediction methods required for the design of Earth-space telecommunication syste*, vol. 8, 2023.

“ITU-R P.839-4,” *Rain height model for prediction methods* , 2013.

A. Usha* and G. Karunakar, “Effects of Different Losses on Satellite Systems,” *International Journal of Recent Technology and Engineering (IJRTE)*, vol. 8, no. 6, pp. 323–326, Mar. 2020.

J. M. Gongora-Torres, C. Vargas-Rosales, A. Aragón-Zavala, and R. Villalpando-Hernandez, “Elevation Angle Characterization for LEO Satellites: First and Second Order Statistics,” *Applied Sciences (Switzerland)*, vol. 13, no. 7, 2023.

H. Bischl *et al.*, “Adaptive coding and modulation for satellite broadband networks: From theory to practice,” *International Journal of Satellite Communications and Networking*, vol. 28, no. 2, 2010.

Rajat Acharya, *Satellite Signal Propagation, Impairments and Mitigation*. 2017.

J. Skarzynski, M. Darmetko, S. Kozlowski, and K. Kurek, “SDR implementation of the receiver of adaptive communication system,” *Radio Sci*, vol. 51, no. 4, 2016.

R. Rinaldo, M. A. Vazquez-Castro, and A. Morello, “DVB-S2 ACM modes for IP and MPEG unicast applications,” *International Journal of Satellite Communications and Networking*, vol. 22, no. 3, 2004.

T. Jaya, E. Gopinathan, and V. Rajendran, “Comparison of BER performance of various adaptive modulation schemes in OFDM systems,” *Indian J Sci Technol*, vol. 9, no. 40, 2016.

E. M. A. Reyouchi, K. Ghoumid, K. Ameziane, and O. El Mrabet, “Performance Analysis of Round Trip Time in Narrowband RF Networks for remote wireless communications,” *Betriebswirtschaftliche Forschung und Praxis*, vol. 7, no. 1, 2017.

S. Ma, Y. C. Chou, H. Zhao, L. Chen, X. Ma, and J. Liu, “Network Characteristics of LEO Satellite Constellations: A Starlink-Based Measurement from End Users,” in *Proceedings - IEEE INFOCOM*, 2023.

T. E. Truman, T. Pering, R. Doering, and R. W. Brodersen, “The InfoPad Multimedia Terminal: A Portable Device for Wireless Information Access Manuscript received 8 Apr. 1997, For information on obtaining reprints of this article, please send e-mail to: tc@computer.org, and reference IEEECS Log Number 104806,” in *Readings in Hardware/Software Co-Design*, Elsevier, 2002, pp. 673–687.

S. Heine, C. Hofmann, and A. Knopp, “End-to-end latency evaluation of LEO satellite IoT systems,” *IET Conference Proceedings*, vol. 2023, no. 48, pp. 216–221, Mar. 2024.

Donal McCarthy, “The Internet from Space: RFIC Advances in High Capacity, Low Latency LEO Satellite User and Ground Terminals,” vol. 56, Nov. 2022, Accessed: Aug. 22, 2025. [Online]. Available: https://www.analog.com/media/en/analog-dialogue/volume-56/number-4/the-internet-from-space-rfic-in-high-capacity-low-latency-leo-satellite-user-and-ground-terminals.pdf

S. Claypool, J. Chung, and M. Claypool, “Comparison of TCP Congestion Control Performance over a Satellite Network,” in *Lecture Notes in Computer Science (including subseries Lecture Notes in Artificial Intelligence and Lecture Notes in Bioinformatics)*, 2021.

G. Maral, M. Bousquet, and Z. Sun, *Satellite Communications Systems*. Wiley, 2020.

S. Van Damme *et al.*, “Impact of Latency on QoE, Performance, and Collaboration in Interactive Multi-User Virtual Reality,” *Applied Sciences (Switzerland)*, vol. 14, no. 6, 2024.

A. Sriraman, S. Liu, S. Gunbay, S. Su, and T. F. Wenisch, “Deconstructing the Tail at Scale Effect Across Network Protocols,” Jul. 2017.

J. Dean and L. A. Barroso, “The tail at scale,” *Commun ACM*, vol. 56, no. 2, 2013.

Stephen Shamakian, “Starlink Grafana Dashboard.” Accessed: Mar. 03, 2024. [Online]. Available: https://github.com/StephenShamakian/Starlink-Grafana-Dashboard